Independent evaluation of conflicting microspherule results from different investigations of the Younger Dryas impact hypothesis

Malcolm A. LeCompte[a,1], Albert C. Goodyear[b], Mark N. Demitroff[c], Dale Batchelor[d], Edward K. Vogel[e], Charles Mooney[d], Barrett N. Rock[f], and Alfred W. Seidel[g]

[a]Center of Excellence in Remote Sensing Education and Research, Elizabeth City State University, Elizabeth City, NC 27921; [b]South Carolina Institute of Archaeology and Anthropology, University of South Carolina, Columbia, SC 29208; [c]Department of Geography, University of Delaware, Newark, DE 19716; [d]Analytical Instrumentation Facility, North Carolina State University, Raleigh, NC 27695; [e]Department of Psychology, University of Oregon, Eugene, OR 97403; [f]Institute for the Study of Earth, Oceans and Space, University of New Hampshire, Durham, NH 03824; and [g]Seidel Research, Camden, NC 27921

Edited by* Steven M. Stanley, University of Hawaii, Honolulu, HI, and approved August 7, 2012 (received for review May 22, 2012)

Firestone et al. sampled sedimentary sequences at many sites across North America, Europe, and Asia [Firestone RB, et al. (2007) *Proc Natl Acad Sci USA* 106:16016–16021]. In sediments dated to the Younger Dryas onset or Boundary (YDB) approximately 12,900 calendar years ago, Firestone et al. reported discovery of markers, including nanodiamonds, aciniform soot, high-temperature melt-glass, and magnetic microspherules attributed to cosmic impacts/airbursts. The microspherules were explained as either cosmic material ablation or terrestrial ejecta from a hypothesized North American impact that initiated the abrupt Younger Dryas cooling, contributed to megafaunal extinctions, and triggered human cultural shifts and population declines. A number of independent groups have confirmed the presence of YDB spherules, but two have not. One of them [Surovell TA, et al. (2009) *Proc Natl Acad Sci USA* 104:18155–18158] collected and analyzed samples from seven YDB sites, purportedly using the same protocol as Firestone et al., but did not find a single spherule in YDB sediments at two previously reported sites. To examine this discrepancy, we conducted an independent blind investigation of two sites common to both studies, and a third site investigated only by Surovell et al. We found abundant YDB microspherules at all three widely separated sites consistent with the results of Firestone et al. and conclude that the analytical protocol employed by Surovell et al. deviated significantly from that of Firestone et al. Morphological and geochemical analyses of YDB spherules suggest they are not cosmic, volcanic, authigenic, or anthropogenic in origin. Instead, they appear to have formed from abrupt melting and quenching of terrestrial materials.

comet | microtektites | Clovis

Manuscript Text

Firestone et al. (1) (hereafter Firestone et al.) proposed that a cosmic impact event occurred at the onset of the Younger Dryas (YD) cooling episode at about 12,900 calendar years Before Present (12.9 ka B.P.). Evidence cited to support their hypothesis includes elevated levels of iron- and silica-rich magnetic spherules, magnetic grains, iridium, and other materials such as nanodiamonds and high temperature melt glass, in association with proxies indicative of biomass burning (1–5). Also reported were charcoal, carbon spherules, aciniform soot, and glass-like carbon. The group further proposed that the impact event may have contributed to the YD cooling episode, the near-contemporaneous extinction of approximately 36 species of megafauna, and triggered significant population declines among some surviving species including human regional populations. The absence of one or more associated impact craters remains problematic. Magnetic spherules, the focus of this paper, were reported by Firestone et al. at or proximal to: a thin sedimentary layer dating to 12.9 ka B.P. called the Younger Dryas Boundary (YDB), found at numerous widely distributed sites in a field extending from California's Channel Islands in the west to Belgium in the east, and from Texas in the south to central Alberta, Canada in the north. Firestone et al. suggested that the spherules represented either ablated impactor material or terrestrial ejecta from one or multiple impacts over North America, centered on the Laurentide Ice Sheet and produced by an extraterrestrial (ET) object or objects whose origin and character remain indeterminate.

The discovery of YDB spherules (1) has produced two significant questions: what is their source and is their abundance and YDB enhancement real? Sedimentary iron- and silica-rich spherules are believed to form from the influx of ET material, directly by meteoritic ablation and indirectly during the sudden cooling of molten terrestrial ejecta from a cosmic impact (6–10). They can also be formed by volcanism, anthropogenic processes, biogenesis, and diagenesis (11, 12) and, in the laboratory, by electrostatic discharge (13). Consequently, determining the nature and origin of observed spherules is essential. Attempts to replicate the spherule abundances and peaks observed by Firestone et al. have produced mixed results. Haynes et al. (14), Mahaney et al. (15), Fayek et al. (16), Israde et al. (4), and Pigati et al. (17) confirmed the presence of YDB spherules, while studies by Surovell et al. (18) and Pinter et al. (19) did not. Surovell et al. examined sediment sequences across the YDB at seven archeological sites in North America, using radiocarbon dates and/or diagnostic cultural artifacts to identify the stratum likely to be the YDB. In all cases, they observed far fewer YDB spherules than reported by Firestone et al. and found no significant abundance peak in spherules at the YDB. At the two sites common to the Firestone et al. study they reported finding not a single spherule in the YDB layer, although in some non-YDB strata, they reported finding extremely low spherule abundances. In producing those results, Surovell et al. asserted their adherence to the magnetic spherule extraction and analysis protocol, dated August 7, 2007, as originally developed by archeologist William Topping, subsequently improved by Allen West, and published in Firestone et al., hereafter referred to as the "protocol." An updated and more detailed protocol was most recently published in Israde et al. (4).

We sought to understand the cause of the discrepant findings of Firestone et al. and Surovell et al. To do so, we limited our

Author contributions: M.A.L., A.C.G., and D.B. designed research; M.A.L., D.B., C.M., B.N.R., and A.W.S. performed research; M.A.L., A.C.G., D.B., and C.M. analyzed data; and M.A.L., A.C.G., M.N.D., E.K.V., and C.M. wrote the paper.

The authors declare no conflict of interest.

*This Direct Submission article had a prearranged editor.

[1]To whom correspondence should be addressed. E-mail: malcolm.lecompte@cerser.ecsu.edu.

See Author Summary on page 17738 (volume 109, number 44).

This article contains supporting information online at www.pnas.org/lookup/suppl/doi:10.1073/pnas.1208603109/-/DCSupplemental.

investigations to three archeological sites, two of which are common to the Firestone et al. and Surovell et al. studies and one site common to that of Surovell et al. Four lines of inquiry defined the scope of our inquiry: (*i*) determining spherule abundances and stratigraphic distribution; (*ii*) analyzing spherule surface morphology using a scanning electron microscope (SEM) photomicrographs and their composition by energy-dispersive x-ray spectroscopy (EDS); (*iii*) comparing the experimental methodologies used; and (*iv*) examining whether microspherule evidence might possess some archeological relevance to the human population decline predicted by Firestone et al. and Anderson et al. (20). To test the population decrease hypothesis, we assumed that if a major YDB spherule abundance peak was identified within or adjacent to strata associated with an apparent disruption in human activity or occupation, then that correspondence would suggest a potential connection.

YDB Sampling Site Information. ***Topper Site, South Carolina.*** Sampling was conducted at the Clovis-aged Topper (TPR) quarry site near Allendale, SC where a complete stratigraphic profile was collected in June 2008 from the surface to 4 cm below a Clovis layer containing extensive debitage, or waste material resulting from stone tool production (*SI Appendix*, Fig. S1). At this site our analyses were limited to four samples of quartz-rich colluvium from 4–10 cm thick across a 31-cm-wide sequence ranging from 52–83 cmbs. These included a 4-cm-thick layer that was centered at 79 cm below the surface (cmbs) and previously accepted as the YDB layer by Firestone et al. and Surovell et al. The others included a contiguous 4 cm sample centered at 83 cmbs, a contiguous 10 cm sample centered at 72 cmbs, and a 10 cm non-contiguous sample centered at 52 cmbs (*SI Appendix*, Fig. S1). These samples were collected within a few meters laterally from those of Surovell et al. and approximately 80 m from those collected by Firestone et al.

At TPR, based on optically stimulated luminescence (OSL) dating (21) and cultural stratigraphy (22), the YDB layer dating to 12.9 ka B.P. is accepted by both Firestone et al. and Surovell et al. as being represented by a few-cm-thick layer containing highly abundant Clovis artifacts and debitage. For approximately 20 cm above the Clovis artifacts, there are extremely few human artifacts, indicating that the quarry experienced a multi-century hiatus in human activity, perhaps as long as 600–1200 y (20), after which the site was reoccupied, as evidenced by the presence of early Archaic Taylor-style points (21). We posited that the stratigraphic position of a peak in spherule abundance might indicate a potential temporal connection between the hypothesized YDB event and quarry dormancy.

Blackwater Draw, New Mexico. From Blackwater Draw (BWD), the type location for the Clovis artifact interval, we acquired four sediment samples varying from 4.5–21 cm in thickness across an 88 cm interval. The samples were taken on January 18, 2006, by the site curator, Joanne Dickenson, from within a protected enclosure called the South Bank Interpretive Center (*SI Appendix*, Fig. S2). Sampled strata include the YDB layer, designated as the "D/C" interface, and identified by the curator as dating to the Clovis period at approximately 12.9 ka B.P., based on extensive radiocarbon dates and the biostratigraphic context of both Clovis artifacts and megafaunal fossils. The layer's age, 12.9 ka B.P., was accepted by both Firestone et al. and Surovell et al. The 5-cm-thick YDB layer is centered at an elevation of 1,238.32 meters above sea level (masl). We also acquired one 21 cm non-contiguous sample below the YDB, centered at 1,237.90 masl, and two 5 cm non-contiguous samples above, one centered at 1,238.41 masl and the other at 1238.78 masl. All samples were collected within less than one meter of the location sampled for the Firestone et al. and Surovell et al. investigations.

Paw Paw Cove, Maryland. On August 8, 2008, we conducted field investigations at the southern end of Paw Paw Cove (PPC) at a proposed Clovis-age site on a westward-facing beach embankment on the Eastern Shore of Chesapeake Bay. We obtained a sample from a stratigraphic section represented by Darrin Lowery, the principal site archaeologist, as most likely to contain YDB proxies, based on his knowledge of the site (*SI Appendix*, Fig. S3). We estimate that our sample was collected within less than a few hundred meters of the site reported in Surovell et al. and includes sediment from the same stratum, as provided to them by Darrin Lowery. Surovell et al. assumed they were sampling the YDB layer, and we have not questioned that assumption; our goal is only to assess whether or not they detected any potential spherules present. One 15-cm-thick stratigraphic sample was extracted, centered at a depth of approximately one meter below the surface. The inferred YDB layer containing nearby Clovis artifacts was located immediately beneath a ubiquitous, orange-colored loess layer that lies atop a noticeably greyish colored stratum (23, 24).

Blind Study. To eliminate potential analytical bias, we participated in a blind test of the sediment samples taken from the two common sites, BWD and TPR. Blind testing was not applicable for the single sample collected from PPC. The eight unprocessed sediment samples, four from each site, were repackaged and distributed by a non-participating third party for blind processing by a member of our group (MAL). The packages were randomly numbered and labeled with the indicated source site, but not with depth or relationship to the YDB layer. At the conclusion of the blind test, we adopted the same chronostratigraphy used by the principal investigators for all of our sites, as well as by Firestone et al. and Surovell et al. YDB depths may vary between studies due to differences in the sampled locations.

Results and Discussion

Magnetic Grain Results. Magnetic grains were extracted from a slurry of the bulk sediment sample, using a grade-52 NdB supermagnet (*Methods*). Overall, we observed some abundance enhancement of magnetic grains at or close to the YDB layer, but the peaks are not unique and are too small to be statistically significant with so few samples. Therefore, we cannot confirm or refute any peak abundance of bulk YDB magnetic grains at either BWD or TPR, as reported by Firestone et al. (Tables 1 and 2), although we did detect a small but consistent increase in the <53-μm grain-size fraction at the YDB for both sites, as discussed below. No conclusions can be drawn from the single sample collected at PPC (Table 3). Whether an increase in bulk- or

Table 1. Topper Quarry Site: Magnetic spherule and grain concentrations relative to stratigraphic position of Clovis debitage (0 cm)

Layer	Depth (cmbs)	Depth relative to debitage (cm)	Sample thickness (cm)	Magnetic Grains (g/kg)	Magnetic Grains (size <53 um) (g/kg)	Magnetic spherule count (#/kg)
Early Holocene	−52	29	10	5.33	0.94	19
Early YD	−72	9	10	5.06	0.63	115
YDB Layer	−79	2	4	5.40	1.12	260
Shadowed by debitage	−83	−2	4	3.97	0.72	30

Table 2. Blackwater Draw Site, NM: Magnetic spherule and grain concentrations relative to stratigraphic position of YDB level in stratum D/C (0 cm)

Layer	Depth (masl)	Depth relative to debitage (cm)	Sample thickness (cm)	Magnetic Grains (g/kg)	Magnetic grains (size <53 um) (g/kg)	Magnetic spherule count (#/kg)
Stratum F	1238.78	45.7	5.0	1.65	0.41	314
Stratum D	1238.41	9.0	4.5	2.21	0.53	1318
Stratum D/C	1238.32	0.0	5.0	2.09	0.63	624
Stratum B/A	1237.90	−42.3	21.0	2.55	0.15	18

small-grain size observed in or immediately adjacent to the YDB layer is statistically significant requires analysis at more sites and samples taken at higher stratigraphic resolution.

Magnetic Spherule Results. For spherule extraction, the Firestone et al. protocol specified sorting the entire magnetic fraction to at least <150-μm, but our initial assessment revealed the outside diameters of nearly all spherules at BWD, PPC, and TPR to be less than 50-μm. Consequently, we separated the magnetic grains into three size fractions based on grain dimensions (d_g): (*i*) $d_g >$ 229 μm with an ASTM #60 sieve; (*ii*) 229 μm > $d_g >$ 53 μm; and (*iii*) $d_g <$ 53 μm with an ASTM #270 sieve. We observed that this additional sorting greatly facilitated spherule detection and counting, as concluded by Israde et al. We determined by spherule counts from these three sites that almost all spherules are <53 μm in diameter. Therefore, we report spherule abundances only from the <53-μm magnetic grain fraction.

To determine spherule abundances in the samples, several portions of approximately 10 mg mass each and of $d_g <$ 53 μm were examined using a reflected-light 180-power optical microscope. The $d_g <$ 53-μm fraction represented from 20–30% of the total magnetic fraction, including grains of all sizes. Photomicrographs were obtained of each candidate spherule observed. Most were then placed manually upon an adhesive tab fixed to an aluminum stub for SEM imaging and EDS analysis to examine their surface morphology, minimize identification ambiguity, and to determine their composition.

Magnetic spherule surface morphology is distinctive when created by processes involving high temperatures followed by rapid cooling, such as during meteoritic atmospheric ablation and impacts (4–12). For identification of spherule surficial morphology (microstructure), we followed the work of Zagurski et al. (25), who used SEM imaging to develop indices of magnetic particles in soil samples extracted from 33 Russian sites. A variety of spherule forms (16 subtypes) were found to be relatively ubiquitous in small concentrations throughout the soil column. The spherules were categorized according to their distinctive polygonal and dendritic surface patterning or microstructures (26) formed by rapid crystallization, indicating they were in a molten state and rapidly quenched (*SI Appendix*, Fig. S4).

Based on SEM analyses, the number of quench-melted spherules was then compared to the number of non-melted spherule candidates, including rounded magnetite grains and authigenic framboids, the latter of which display blocky crystals formed by slow crystallization (*SI Appendix*, Fig. S5). The ratio between the SEM-verified melted spherules and the total candidate spherules provided what we call a false-positive correction factor for each layer.

The numbers of spherules in each 10-mg portion were found to vary enough to prompt examination of multiple 10-mg aliquots to more accurately establish spherule abundances at each stratigraphic level. To assure statistical significance, we continued to search for spherules until a minimum of six candidates in each layer were confirmed as melted spherules. In Fig. 1, six confirmed melted spherules are shown each for TPR and PPC, with 30 confirmed spherules for BWD. These spherules exhibit the surface microstructures, which are consistent with formation by melting at high temperatures, followed by rapid quenching. We summed the total number of candidate-spherules per unit mass of magnetic grains in each layer and then multiplied that times the false-positive correction factor. The factor for both BWD and PPC is 0.8, meaning that 20% of candidates were rejected. For TPR, the factor was 0.25, meaning the 75% of candidates were rejected, many because they were apparently framboids. Last, we calculated total spherule abundance by normalizing the corrected value to yield the number of quench-melted spherules per kilogram of bulk sediment. SEM micrograph validation was only applied to those spherules found in or immediately above the YDB layer. For the stratigraphically highest and lowest samples, no SEM work was performed. The total number of uncorrected candidate-spherules is reported as an upper limit. The actual spherule values are almost certainly lower. In summary, we found that SEM analyses to determine microstructure and the application of a correction factor are essential, because true YDB spherules cannot be reliably identified by light microscopy alone as was attempted by Surovell et al., Pinter et al., and Pigati et al. (17).

Topper Spherules. At the TPR Paleoindian quarry, we removed sediment lying directly on top of the layer of debitage (Fig. 2 and *SI Appendix*, Fig. S1), which delineated the level of highest Clovis usage of the quarry. Immediately above it there is almost no debitage. Next we lifted off selected pieces of Clovis debitage

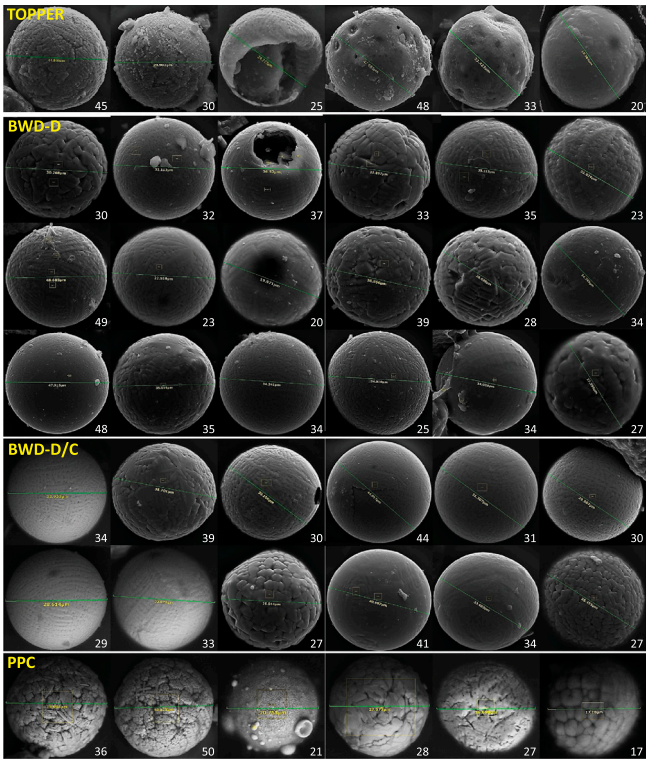

Fig. 1. Spherules picked from the YDB layer at each of the three sites. BWD also exhibited abundant spherules in the D stratum just above the YDB (D/C stratum). We found statistically significant numbers of spherules in the YDB at all three sites, whereas Surovell et al. found none. White numbers at bottom right represent diameter of spherules in microns (μm).

Fig. 2. Topper site, SC. Tariq Ghaffar, Public Broadcasting System's Time Team America archeologist, excavating pedestals (lower arrow) capped by debitage (upper arrow) at the TPR SC Clovis quarry Archeological site. YDB layer indicated by dotted line. Samples were collected from immediately above and immediately below selected pieces of debitage. Photo from Al Goodyear and Meg Galliard.

and carefully collected the sediment directly beneath each chert fragment.

For the sediment atop the debitage, two aliquots were examined of the small magnetic grain fraction <53 μm), which represented 20% of the total magnetic aliquot that weighed approximately 65 mg. One aliquot of 13 mg yielded 14 spherule candidates and a second aliquot of 30 mg yielded 10 candidates. SEM examination indicated that many of these were framboids so were excluded. The other spherules exhibited surface microstructures indicative of rapid melting and quenching as described by previous researchers (25–27). Spherule sizes at TPR range from 25 to 45 μm, averaging approximately 30 μm, and they are geochemically and morphologically similar to YDB spherules extracted from the other two sites.

Spherule concentrations exhibit a significant peak of approximately 260 spherules/kg in the 4-cm-thick YDB layer immediately above the debitage (Fig. 3, Table 1). For the 4-cm-thick sediment layer immediately underlying or shadowed by fragments of chert débitage and centered 2 cm below the debitage layer there is a significant decrease to about 30 candidate-spherules/kg (false-positive correction yields 8 spherules/kg). In the 5-cm-thick sample centered at 9 cm above the debitage layer there are 115 spherules/kg and the layer approximately 29 cm above the debitage strata contained an estimated 31 non-corrected candidate-spherules/kg. Table 1 shows that the lowest spherule abundance occurs just beneath the YDB layer and coincides with inferred high quarry usage during Clovis times. The highest spherule abundance appears in the YDB layer, contemporary with the inferred abandonment of the quarry, consistent with evidence for a population decline posited by Firestone et al. and Anderson et al. (20).

Blackwater Draw Spherules. At BWD the D/C stratum was accepted by both Firestone et al. and Surovell et al. as the YDB layer. A sample collected from that stratum produced approxi-

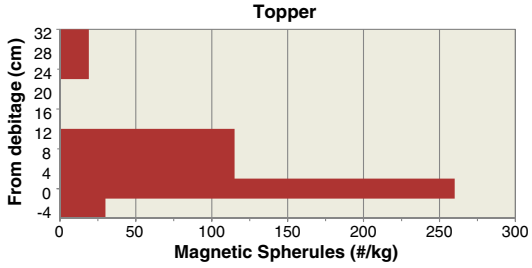

Fig. 3. Topper site. Graph showing the stratigraphic distribution of magnetic spherule concentrations in the <53-μm grain-size fraction. Clovis debitage is at 0 cm. The 4 cm YDB level is centered 2 cm above it.

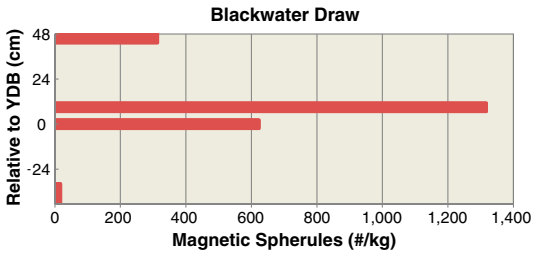

Fig. 4. Blackwater Draw site, NM. Graph showing the stratigraphic distribution of magnetic spherule concentrations in the <53-μm grain-size fraction. YDB level is centered at 0 cm.

mately 25 spherules from 34 mg of the d_g < 53-μm magnetic fraction representing 28% of the total 120-mg magnetic aliquot. SEM-confirmed spherules totaled about 624 spherules/kg (Fig. 4, Table 2). This compares to approximately 36 spherules from 17 mg in the D stratum centered 10 cm above the D/C stratum for a total of 1,318 spherules/kg. Spherule sizes in the two layers varied between 17–50 μm, averaging 30 μm. In contrast to TPR, where our results appear to support the existence of a distinct and relatively narrow abundance peak in strata at the YDB, BWD spherule abundances appear to exhibit a broader abundance peak of about 20 cm width just above the YDB stratum. At −40 cm, the D/C stratum spherule abundance is distinctly lower at 18 candidate-spherules/kg, while at +40 cm, candidate-spherule abundance is at approximately 314 spherules/kg. Enhanced spherule abundance of the layers overlying the YDB layer may be due to enrichment by fluvial action as suggested by Haynes et al. or slightly later deposition.

Paw Paw Cove Spherules. The size range of spherules extracted from the single PPC sample of YDB age ranged from 20–49 μm, averaging 30 μm. Total abundance was 317 spherules/kg. Seven spherules were extracted from 32 mg of the d_g < 53-μm fraction, representing 27% of the total magnetic aliquot weighing approximately 289 mg. Examination by both optical microscopy and SEM revealed the spherules to be generally similar to those extracted from the BWD and TPR sites. Nearly all spherules examined were found to be rich in titanium, whereas such spherules were found to be rarer at the other two sites, amounting to approximately 20% of total spherules. One spherule was found to be enriched in iron and the rare earth elements (REEs), cerium (22%), and lanthanum (10%), along with praseodymium and neodymium as discussed below. Because the sample was extracted from a cleaned cutbank at depth, anthropogenic sources are considered unlikely but cannot be completely ruled out.

Spherule Geochemical Analyses. Geochemical analyses of many spherule candidates from each site were performed at North Carolina State University's Analytical Instrumentation Facility using a Hitachi S3200 Variable Pressure SEM with EDS capability. Tables summarizing the elemental and oxide abundances of these spherules are presented in *SI Appendix*, Tables S1–S3. Spectrographic and major oxide abundances for representative magnetic spherules are shown below for each site. Each figure also combines an optical photomicrograph at 180-power magnification with an associated SEM micrograph.

For TPR, 11 EDS analyses were performed on spherules yielding averages of 61 wt % FeO, 12 wt % Al_2O_3, 17 wt % SiO_2, and 8 wt % TiO_2; all other oxides were <2 wt%. These values are consistent with average percentages for sediment at the Earth's surface, indicating that these spherules formed from melted terrestrial surficial sediments (*SI Appendix*, Table S1). Of the 11 EDS analyses, seven showed enrichments in iron (>53 wt%), two were titanium-rich (>34 wt%), and three were silica-rich (>27 wt%) (*SI Appendix*, Table S1). The TPR spherule shown in the SEM image in Fig. 5 exhibits a relatively dull finish due

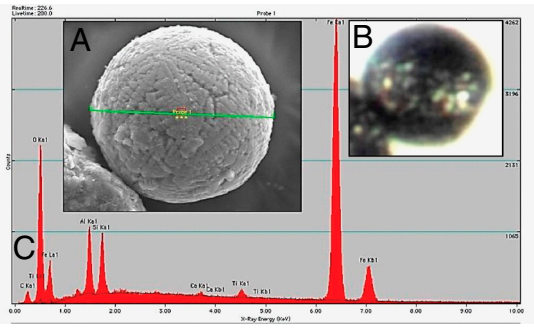

FeO	Al_2O_3	MgO	CaO	SiO_2	K_2O	Na_2O	TiO_2	P_2O_5	MnO	Cr_2O_3	NiO	SO_3
83.61	8.17	0.06	0.26	4.53	0.00	0.11	0.52	2.32	0.00	0.00	0.02	0.40

Fig. 5. TPR 45-μm diameter spherule (TU2-Sph-3-110505) extracted from sediment in immediate contact with Clovis age debitage. (*A*) SEM image; (*B*) optical photomicrograph; and (*C*) EDS spectrum and elemental oxide abundances.

to its rough faceting, suggestive of a Zagurski index identifier "polygonal granular" (S^{pgr}) (25). The dull, somewhat flattened surface shown in the optical photomicrograph is likely due to a perforated surface around a hollow interior. Departures from perfect sphericity are common, thus the only reliable approach of verifying that a candidate is a true spherule is by using SEM-EDS analysis to examine its surface morphology and geochemistry.

For BWD, 52 EDS analyses were performed on YDB spherules yielding averages of 85 wt % FeO, 2 wt % Al_2O_3, 3 wt % SiO_2, and 7 wt % TiO_2; all other oxides were <2 wt%. These values are similar to average percentages for sediments at the Earth's surface, indicating that these spherules formed from melted terrestrial surficial sediments (*SI Appendix*, Table S2). Of the 52 EDS analyses, 45 showed enrichments in iron (>55 wt%), seven were titanium-rich (>31 wt%), and none were silica-rich (>50 wt%) (*SI Appendix*, Table S2). The BWD microspherule shown in Fig. 6 exhibits a dendritic quench-textured microstructure suggestive of the Zagurski index identifier "grooved" (S^{g}) (25). The predominately iron oxide composition of this spherule, shown in Fig. 6, is similar to that of the TPR spherule in Fig. 5. Essentially all of the BWD spherules display surface features indicative of rapid melting and quenching that produced distinctive microstructures. Most appear similar to Zagurski index identifiers "grooved" (S^{g}) and "ordered granular" (S^{ogr}) (25). Approximately 5% have surface features similar to either Zagurski index identifier "polygonal granular" (S^{pgr}) or "sinuous patterned" (S^{s}) (25).

For PPC, eight EDS analyses were performed on six YDB spherules yielding averages of 40% FeO, 5% Al_2O_3, 2% MgO, 3% SiO_2, 2% Na_2O, 30% TiO_2, and 2% Mn_2O_7; all other oxides were <2%. These values reasonably match average percentages for sediments at the Earth's surface indicating that these spherules formed from melted terrestrial surficial sediments (*SI Appendix*, Table S3). Of the eight EDS analyses, one was enriched in iron (>51 wt%), five were titanium-rich (>39 wt%), and none were silica-rich (>4 wt%) (*SI Appendix*, Table S2). Five of the six spherules investigated (83% of the total) were found to be titanium-rich, a much higher percentage than those from both TPR and BWD where values of 20% total were more typical. Fig. 7 shows an SEM and optical microscopic image of a PPC titanium-rich spherule.

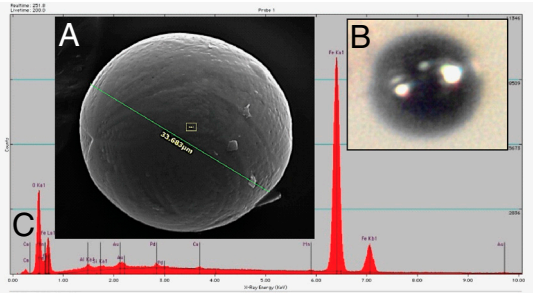

FeO	Al_2O_3	MgO	CaO	SiO_2	K_2O	Na_2O	TiO_2	P_2O_5	MnO	Cr_2O_3	NiO	SO_3
95.39	2.16	0.50	0.21	0.84	0.00	0.32	0.01	0.17	0.38	0.00	0.02	0.00

Fig. 6. BWD 34-μm-diameter spherule (BWD-DC-Sph-5-110314) extracted from the D/C stratum that contains Clovis artifacts. (*A*) SEM image; (*B*) optical photomicrograph; and (*C*) EDS spectrum and elemental oxide abundances.

Another spherule (Fig. 8) exhibits a relatively smooth surface that is enriched in the rare earth elements (REEs) cerium and lanthanum. This PPC spherule's shape is not perfectly spherical. Its surface may have experienced either volatile eruptive outgassing or accretionary collision of multiple spherules causing numerous hemispherical mounds of various sizes. One of these mounds appears as an inverted cup-shaped structure. It and other surface mounds are enriched in REEs praseodymium and neodymium. The surficial cup-shaped structure may be indicative of a partially collapsed bubble, perhaps due to out-gassing and deflation of the spherule while molten.

Focused ion beam (FIB) sectioning of the REE-rich spherule from PPC revealed a 10-μm-diameter spherical void with its center displaced toward a prominent bulge (Figs. 8 and 9). The chemical compositions of the inner crust and interior are similar to that of the exterior. Differences in iron abundances account for the dark and light portions of the patterned interior. EDS analysis revealed an elemental composition rich in REEs including lanthanum (10%), cerium (20%) with trace amounts of praseodymium and neodymium, which are not typical elemental components of surficial rocks in the Maryland region (27). Although this unusual spherule may be an atypical anthropogenic contaminant, REEs are also well-known constituents of cosmic material, especially chondritic meteorites (28–30). Previous studies have reported elevated levels of REEs also in association with the YDB in North America and Europe* (1).

Framboidal Spherules. Pinter et al. examined YDB sediment at a site not previously tested for spherules and suggested that Firestone et al. misidentified framboids as spherules. Framboids are formed by slow crystal growth and so do not possess the distinctive surface microstructures found on YDB magnetic microspherules and are therefore easily differentiated. A typical spherical framboid is shown in *SI Appendix*, Fig. S5. Framboids were observed but perceived to be rare at both the BWD and PPC sites where no attempt to quantify their abundance was made. At TPR, framboids are very abundant in the YDB layer, approximately ≥1000 per kg, decreasing above and below. It is unclear why both spherules and framboids exhibit highest abundances in the YDB at this site.

Comparison of Protocols Used by Surovell et al. and Firestone et al. Surovell et al. purportedly used the same protocol as Firestone et al. yet were unable to find a single spherule in YDB sediments at three previously reported sites. They concluded that the "discrepancy between the two studies is particularly troublesome." Our investigation reveals the abundant presence of YDB spherules at all three widely separated sites, consistent with the results by Firestone et al. Because of this difference we now examine the methodology of Surovell et al. who reported their methods in detail. Comparing the methodology of each, we find Surovell et al. deviated substantially in several critical aspects, and we suggest that this departure resulted in their finding no YDB spherules

*Andronikov AV, Lauretta DS, Andronikva IE, Maxwell RJ (2011) On the possibility of a late Pleistocene, extraterrestrial impact: LA-ICP-MS Analysis of the Black Mat and Usselo Horizon Samples, Abstract for a poster presented at the 74th Meteoritical Society Meeting, held in London U.K., August 8–12, 2011.

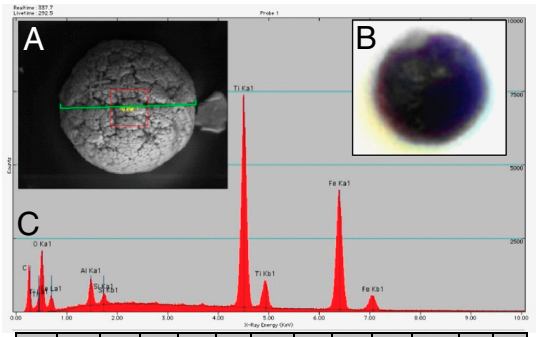

FeO	Al_2O_3	MgO	CaO	SiO_2	K_2O	Na_2O	TiO_2	P_2O_5	MnO	Cr_2O_3	NiO	SO_3
41.00	6.83	0.67	0.12	2.59	0.05	0.61	47.5	0.12	0.01	0.01	0.00	0.45

Fig. 7. PPC 50-μm-diameter spherule (PPC-YDB-Sph-4-50mic-100707) extracted from sediment at a depth accepted as coeval with the YDB. (*A*) SEM image; (*B*) optical photomicrograph; and (*C*) EDS spectrum and elemental oxide abundances.

at these three sites. A summary comparison of the three protocols is in *SI Appendix*, Table S4.

We have identified five major deficiencies that contributed to the negative results reported by Surovell et al.

1. *Deficiency: YDB Layer Sample Thickness*. Source: Firestone et al. "we found a thin, sedimentary layer (usually <5 cm)." Source: Surovell et al. "*SI Appendix*, Table S1 displays seven sites at which the YDB layer ranges from 5–28 cm, averaging 11 cm."

   Firestone et al. identified the YDB as being a thin layer containing increased abundances of markers and collected samples at seven main sites with YDB thicknesses ranging from 0.5–5 cm, averaging 2.3 cm. Surovell et al. collected thicker samples ranging from 5–28 cm thick, averaging 11 cm, which are nearly five times as thick. Consequently spherule abundance would be diluted making them more difficult to detect. For comparison our YDB sample at TPR was collected as a 4-cm-thick sample while Surovell et al.'s was 10-cm-thick. In five of seven instances Surovell et al. collected samples of ≥10 cm thickness. Although this is thicker than recommended we do not consider this to represent a major flaw by itself. However, it becomes of greater potential importance when combined with other deviations from the protocol of Firestone et al.
2. *Deficiency: Inadequate Aliquot Size*. Source: Firestone et al. Protocol: they analyzed "one or more 100–200 mg aliquots…. Microspherules are usually rare, often making it necessary to inspect the entire magnetic fraction." Source: Surovell et al. "examined 10–40 mg…per sample," and did not investigate the entire magnetic fraction of any sample.

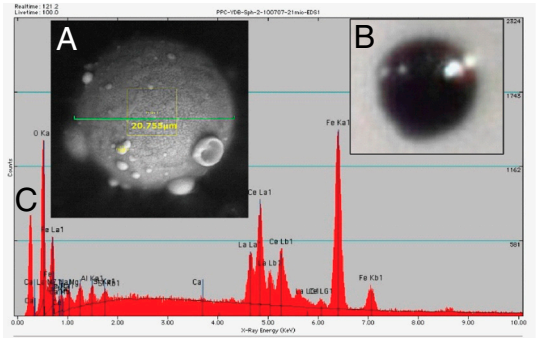

FeO	Al_2O_3	MgO	CaO	SiO_2	K_2O	Na_2O	TiO_2	P_2O_5	MnO	Cr_2O_3	NiO	SO_3	La_2O_3	CeO_2
48.24	4.79	6.11	0.12	2.66	0.03	4.90	0.03	0.00	0.84	0.12	0.01	0.21	10.10	21.83

Fig. 8. PPC 21-μm-diameter spherule (PPC-Sph-2-21 mic-100707) extracted from a level in the sequence accepted to be coeval with the YDB. Note high abundances of REEs. (*A*) SEM image; (*B*) 180-power optical photomicrograph; and (*C*) EDS spectrum and elemental oxide abundances.

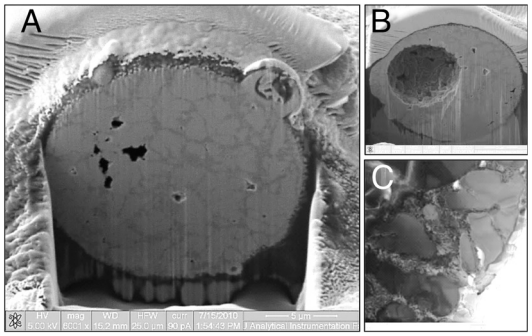

Fig. 9. Mosaic of SEM images of the interior structure of REE-rich YDB spherule from PPC (PPC-Sph-2-21 mic-100707) after FIB thin-sectioning (*A* and *B*). Accretionary surface-layer texture (*C*) is revealed by TEM of thin-section.

The amount of magnetic grains that Surovell et al. examined was inadequate to be statistically significant, invalidating any conclusions regarding spherule abundances. Surovell et al. examined from 20–100 times smaller aliquots of the magnetic fraction than did Firestone et al. with the result that they found no spherules in five-out-of-seven YDB layers. This deficiency is a major contributor to their reported lack of spherules, because the aliquots analyzed by Surovell et al. were of insufficient size to visually detect even a single spherule. To illustrate the consequences of that deficiency, consider our results from TPR, where we estimated 260 spherules in 5.40 grams (or 5,400 mg) of magnetic grains. This amounts to approximately two spherules in every 40 mg, the maximum amount that Surovell et al. analyzed. Without some means of amplifying the detectability of those two spherules, it seems unlikely that Surovell et al. would have detected even a single spherule, and, indeed, they reported finding none.

3. *Deficiency: Size-Sorting of Grains*. Source: Firestone et al. Protocol: "We used ASTM sieves to screen the magnetic grains into separate fractions and worked mostly with the <150-μm samples." Source: Surovell et al. "…[samples] were passed through a #18 one-mm sieve."

   Size-sorting of the extracted magnetic grains is essential to overcome the difficulty in detecting rare spherules among the far more numerous, non-spherical magnetic grains. To illustrate that difficulty, consider again our results from TPR, where we estimate 260 spherules in 5.40 grams of magnetic grains for every kilogram of sediment. Assuming a linear grain size distribution and spherical grains for simplicity, we estimate there may be roughly 2.5 million discrete magnetic particles in those 5.40 grams, resulting in a ratio of spherules to grains of approximately 1:10,000. Our spherule counts indicate that the portion containing the smallest grains (<53 μm) accounts for 90% of the total spherule abundance. Thus, eliminating larger grains greatly reduces the probability of these obscuring small spherules and also enhances spherule prevalence, making spherules easier to detect. Although careful counting might overcome this problem, it is better to follow the prescribed protocol to increase accuracy of counts.

   Size-sorting also addresses a more serious problem, which is to overcome the downward migration of microspherules, also known as "downward fining." This phenomenon, well-known in sedimentology, is the process by which agitation of sediment results in fine particles preferentially migrating downward through the voids between larger grains, thereby concentrating larger grains at the top and smaller grains at the bottom of a container (31). This phenomenon is particularly applicable to spherule counting, because spherules tend to be much smaller on average than non-spherulitic magnetic grains. Size-sorting counters downward fining. We also found that it is vitally important to thoroughly mix and evenly split each size-sorted

portion on a smooth impervious surface as a last step prior to selecting an aliquot for spherule counting. Even so, there may yet be normal but acceptable variation between aliquots. Neglecting to size-sort, an investigator might extract a small aliquot of unsorted, spherule-depleted material from the top of a container. The end result is the mistaken conclusion that spherules are absent from the entire magnetic sample, whereas they are only absent from the top of the container. Based on the published methodology adopted by Surovell et al., we suggest that their study may have suffered from this effect because size-sorting was not conducted.

Finding a single spherule among 10,000 magnetic grains is such a tedious endeavor that some have claimed that any results may be highly subjective and therefore unreliable (14). In light of the above difficulties, we considered whether magnetic spherule counting is a quantitative science, or rather, a subjective art as suggested by Haynes et al. (14). Cognitive neuroscience might reveal whether limitations in human perception affect the ability of an operator to discriminate spherules among numerous non-spherulitic distractors. Several factors are known to contribute to successful target detection amongst numerous distractors, including distractor abundance, heterogeneity, target prevalence, and discriminability (32, 33). Each of these factors may play some role in accurately measuring the number of target-spherules. For example, visual search for infrequent targets ($\leq$1% prevalence) is known to be highly error-prone, resulting in >30% of targets being missed altogether (34). Because spherule prevalence in magnetic fractions is often extremely low (0.006%–0.125%), visual searches are likely to be error prone with target misses common. Also, magnetic distractor grains tend to be sub-rounded with surface finish and color very similar to the often silvery-black, glossy surfaced, spherules. This similarity, coupled with the rarity of spherules, leads to a demanding visual search that could plausibly produce a severe underestimate of target numbers.

To help counter these inherent search difficulties, size-sorting eliminates the largest grains in the search set and improves visual search performance in two fundamental ways. First, it decreases the number of distractors. For example, if the relative abundance of the smaller grains is low (20% of the total grain-mass), then size-sorting removes many distractors (80% of grain-mass), significantly improving target prevalence. Second, size-sorting minimizes the size disparity between targets and distractors. Although it may appear counterintuitive, distractors that are highly dissimilar to one another generally produces a slow and effortful search (e.g., finding a red target amongst blue, yellow, purple, and green distractors). By contrast, when distractors are more similar to each other, search becomes dramatically easier. Targets tend to pop out from the homogeneous set of distractors (e.g., finding red targets amongst many purple distractors) (32, 35). This effect becomes more evident as size homogeneity increases. Consequently, the exclusion of the large grains is likely to greatly reduce the perceptual demands of the search task, leading to a substantially more accurate measurement of spherule abundances.

Cognitive neuroscience thus indicates there are significant difficulties inherent in spherule detection that require mitigation to reduce process subjectivity. Even after minimizing difficulties, it is reasonable to expect variation in results (e.g., from operator error), even amongst researchers using the same protocol. Indeed, we found that analyzing successive aliquots from the same magnetic fraction produced variations up to $\pm$50%. However, researchers adhering to a rigorous protocol that includes size-sorting have a greater chance of overcoming the inherent difficulties of such a search. Our results are sufficiently similar to those of Firestone et al. to suggest that spherule detection is replicable to at least within $\pm$50%, and therefore, refuting the speculation that spherule detection is strictly subjective. Researchers routinely quantify spherules in ocean sediments and in ice cores with reproducible results (26).

It is noteworthy that when we began this investigation, we inadvertently failed to size-sort the magnetic fraction from some of these sites. As a result, we initially found no spherules at all, consistent with the results of Surovell et al. However, once we implemented rigorous size-sorting, we observed spherules in large numbers consistent with Firestone et al.

4. *Deficiency: Perfect Sphericity*. Source: In Fig. 2 of Firestone et al., two of the four spherules in that figure are clearly somewhat oval-shaped and non-spherical. Source: Surovell et al., they decided to "eliminate a number of particles that at first glance appeared to be highly spherical but were not."

These quotes demonstrate that Surovell et al. deviated from the Firestone et al. protocol by independently devising a more restrictive optical criteria for selecting spherule candidates. Surovell et al. limited the spherule count to only those particles matching an extreme degree of sphericity, even though both the protocol and spherule images published by Firestone et al. and others indicate that spherules commonly deviate from perfect sphericity (36–40). By incorporating such a condition into their protocol, Surovell et al. would most likely have rejected candidates such as the rough spherules shown in Figs. 5 and 7, as well as the lumpy spherule rich in REEs found at PPC (Fig. 8). Many spherules have conspicuous punctures in their shell-like surface as revealed in SEM images, as well as other flaws that reduce their apparent sphericity and reflectivity. Even so, each exhibits the characteristic quench-melted dendritic texture that is characteristic of YDB spherules and that differentiates them from framboids or detrital grains. We include a mosaic of SEM images of representative YDB spherules (Fig. 1) to verify that spherules we counted were consistent with the original Firestone et al. protocol under which Surovell et al. operated. Our spherule abundances are based upon the SEM confirmation of spherule candidates. We used a conservative identification protocol to select spherule candidates similar to but not quite as restrictive as that employed by Surovell et al. This included high-surface reflectivity and approximate sphericity based on overhead illumination. Nevertheless, we found it essential to use the SEM to verify a candidate spherule's true nature. Based on our results from light microscopy and SEM, we find that perfect sphericity is not necessarily a defining characteristic of YDB spherules, and so, because Surovell et al. utilized this additional step, it is possible they eliminated a significant percentage of YDB spherules present.

5. *Deficiency: No Geochemical Analyses*. Source: Firestone et al. Protocol: "Selected microspherules were mounted, sectioned, and analyzed by XRF [EDS] and/or laser ablation." Source: Surovell et al., [no spherules were geochemically analyzed].

Without SEM imagery to examine their surface microstructure, it is impossible to differentiate YDB magnetic spherules from those created by other natural or anthropogenic sources including framboids or rounded detrital magnetite, which, in our experience, often appear identical to YDB spherules under an optical microscope. Firestone et al. examined selected YDB magnetic spherules with SEM imaging but, unfortunately, published only optical micrographs and EDS analyses. SEM imagery shows magnetic spherule surface morphology due to meteoritic ablation, terrestrial impact or anthropogenic ejecta to be essentially identical (38–40). EDS analyses provides information to distinguish among them. It is impossible to infer the origin of cosmic, volcanic, anthropogenic, or impact spherules by visual identification alone[†]. It is essential to conduct geochemical analyses and compare the results with that from known spherule populations.

[†]Buchner E, Schmeider M, Strasser A, Krochert L (2009) Impacts on spherules. MAPS 40th LPSC, paper 1017.

For example, Pigati et al. (17) reported candidate YDB spherules at Murray Springs, AZ, confirming the abundance results of Haynes et al. (14) and Firestone et al., but also reported abundant non-YDB spherules in Chile. However, they performed no SEM or EDS analyses to determine the morphological and geochemical characteristics of any spherules within and outside the YDB layer. Since their non-YDB sampling sites in Chile are within a few kilometers of dozens of active volcanoes, it is almost certain that they observed numerous volcanic spherules and possibly none due to impact. Because those authors did not perform SEM imaging and EDS analyses, it is impossible for them to reach reliable conclusions about what they found.

Surovell et al. did not perform SEM imaging or geochemical analyses, and yet, like Pigati et al., asserted that all magnetic spherules are cosmic in origin. Pinter et al. and Haynes et al. did not report the results of their spherule SEM analyses and likewise concluded spherules were of cosmic origin without supporting data. Lacking SEM imaging and/or EDS analyses, the accuracy of their spherule counts and speculations about origin are highly suspect. As an example of this, Pinter et al. reported observing large numbers of framboids and detrital magnetite well outside the YDB and then speculated that most YDB spherules are simply these other particles. Our results and images indicate their claim to be unfounded. There are fundamental and easily observed differences between quench-melted spherules, unmelted detrital magnetite, and authigenic framboids.

The EDS results of our study are consistent with those of Firestone et al. that YDB spherules do not appear to be of cosmic origin. Spherule composition is shown plotted on a ternary diagram (Fig. 10*A*) that compares normalized molar percentages of magnesium, iron, and titanium oxides observed in 276 cosmic microspherules collected in Antarctic ice (41) with 85 spherules from TPR, BWD, and PPC. The results demonstrate that cosmic spherules typically are enriched in MgO, as confirmed by Taylor et al. (41), in contrast to YDB spherules that are depleted. Also, cosmic spherules typically are depleted in TiO_2, while YDB spherules are TiO_2 enriched. Thus, YDB spherules are geochemically distinctive and dissimilar to cosmic spherules. Regarding other potential origins, the spherules we observed are unlikely to be of anthropogenic origin because: (*i*) they were buried at sufficient depths to preclude downward contamination of modern spherules; and (*ii*) they exhibit abundances peaking at approximately 12.9 ka. Also, a volcanic source is unlikely because we detected no volcanic materials such as ash and tephra in any YDB layer examined. It seems unlikely that abundant volcanic spherules would persist in sediment without abundant ash or tephra.

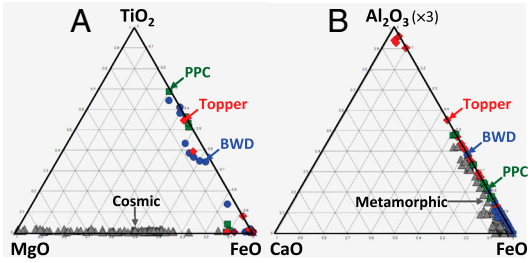

Fig. 10. Ternary diagrams comparing the geochemistry of spherules collected from TPR (red diamonds), BWD (blue circles) and PPC (green squares) with (*A*) cosmic spherules (black triangles) (source: Taylor et al.,) and (*B*) terrestrial undifferentiated metamorphic rocks (source: USGS, 2001). All but a few spherules from TPR are similar to metamorphic minerals. In summary, YDB spherules do not resemble cosmic spherules, but instead appear consistent with formation by a high-energy source requiring the melting of terrestrial sediment.

Firestone et al. proposed that some YDB spherules most likely formed from the melting of terrestrial sediments. We investigated that hypothesis by comparing the geochemistry of YDB spherules with terrestrial metamorphic rocks. The results are shown in an aluminum-calcium-iron ternary diagram (Fig. 10*B*) plotting the normalized molar percentages of calcium, iron, and aluminum oxides resulting from 85 EDS analyses of spherules collected from TPR, BWD, and PPC. These data are compared to 115 samples of undifferentiated metamorphic rocks, including schist and shales from 12 U.S. states, mostly in the Northeast and Midwest, as compiled by the USGS in their PLUTO database (42). These results demonstrate geochemical similarity between YDB spherules and metamorphic rocks, supporting the hypothesis of Firestone et al. that YDB spherules likely formed from melted terrestrial rocks. Furthermore, the spherules were originally in a molten state, as confirmed by our SEM imagery exhibiting surface textures characteristic of quench-textured molten droplets (25). Various YDB spherules observed are comprised of FeO at a maximum of 99% or SiO_2 at 64% or TiO_2 at 58% (*SI Appendix*, Tables S1–S3). These percentages imply a range of formation temperatures that includes 1550 °C (the melting point of FeO), 1650 °C (the melting point of TiO_2), and 1730 °C (the melting point of SiO_2). The high temperatures inferred from the YDB spherules' microstructures are consistent with the melting and rapid cooling of an energetic and transient process. The spherule's wide spatial distribution might be due to a small number of very energetic event(s) or very many dispersed events of lesser magnitude. Based on spherule stratigraphy, we speculate that spherule deposition occurred over a brief period, temporally proximate to the YD onset. At some sites, spherule abundance may have experienced subsequent enhancement due to environmental processes (e.g., deflation).

Human Population Decline. Firestone et al. proposed that the YDB impact triggered a decline in Clovis populations at 12.9 ka B.P. and, subsequently, Anderson et al. (20) provided three lines of evidence in support of a human decline at multiple sites in North America, including the TPR site, as well as Europe and elsewhere. That hypothesis led us to investigate whether YDB microspherule results at the sites we examined could shed light on this issue.

First, the Clovis-age YDB layer at BWD has been clearly identified by the distribution of megafaunal remains and Clovis artifacts, and a hand-dug Clovis well (43). At the sample collection site, Folsom artifacts lie above an archeological gap zone that is 10–20 cm thick and lying immediately above the Clovis layer. This culturally dead zone, which extends discontinuously across the 157-acre site, has no known Folsom artifacts in contact with Clovis artifacts indicating a post-Clovis occupational hiatus of 200–600 y (19). The presence of this archeological gap is consistent with the proposed population decline.

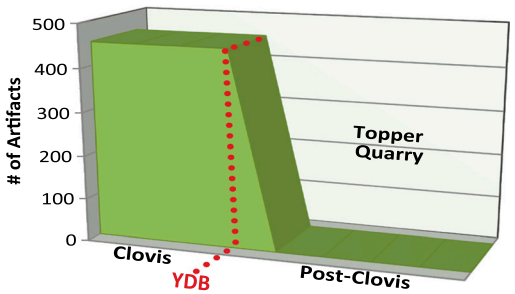

Fig. 11. Graph depicting distribution of total-known Clovis artifacts (n = 453 of projectile points, preforms, blades, and cores) compared to post-Clovis (n = 1 point), a decline in quarry usage of >99% that persisted for approximately 600 y (*SI Appendix*, Table S5; data from Anderson et al. 2011).

Table 3. Paw Paw Cove, MD: Magnetic spherule and grain concentrations in YDB

Layer	Depth (cmbs)	Depth relative to YDB (cm)	Sample thickness (cm)	Magnetic grains (g/kg)	Magnetic grains (size <53 um) (g/kg)	Magnetic spherule count (#/kg)
YDB Layer	~100	0	15	3.64	1.125	317

At PPC, on the Delmarva Peninsula, Befell et al. (44) presented data indicating that beginning at the YD onset at 12.9 ka B.P. and continuing for 1,400 y the Potomac River-Chesapeake Bay area was abandoned by humans. This also appears to be the case at PPC, where the Clovis horizon is overlain by loess-derived strata tens of centimeters thick that was deposited after the YD onset and contains no reported human artifacts. As at BWD, these results are consistent with a post-YDB population decline.

At TPR, low abundances of candidate spherules (≤30/kg) coincide with the debitage layer that was formed during the occupation of Clovis peoples (Fig. 3 and Table 1). This was followed by a significant increase in YDB spherule abundance (260/kg) just above the debitage layer. We call this the "chert shadow effect." It coincided with the almost complete disappearance of Clovis artifacts, suggesting human abandonment of the quarry (Fig. 11) that is roughly coeval with spherule deposition. The observed archeological gap lasted for approximately 600 y or longer (19). Because the quarry was a regionally important sources of high-quality chert, it seems unlikely that the quarry would have become dormant if the local population had remained unchanged. Thus, our data appears consistent with a population decline. The time of quarry dormancy appears to coincide with whatever phenomena created and deposited the spherules. However, Buchanan et al. (45) and Holiday et al. (2010) (46) find no evidence to support a population decline.

Correlation of Three Test Sites. For magnetic grains we found densities equal to or higher than the values reported by Firestone et al. and higher than those of Surovell et al. at all three sites sampled. For confirmed YDB spherules the comparison abundances are summarized for all three sites in Table 4. Our data are consistent with those of Firestone et al. and inconsistent with those of Surovell et al., who found no magnetic spherules in YDB strata at the three sites. However, the relatively high concentrations we report at all sites could have resulted from our use of a 25% stronger magnet (N52) and thinner plastic bags (2–3 mil), leading to increased recovery rates. In our opinion these differences in methodology are insufficient to account for the complete absence of magnetic spherules reported by Surovell et al. From their published protocol it is clear that they did not sufficiently adhere to the protocol of Firestone et al. for extraction of magnetic spherules. Nevertheless, we find in agreement with Surovell et al. that magnetic-grain concentrations alone are not a reliable proxy for accurate identification of the YDB layer. At BWD the magnetic grain abundance peaks slightly above the YDB layer and, while grains do peak at the YDB at TPR, concentrations are similar to that found in overlying strata. However, if the magnetic grains are size-sorted and weighed, the abundances of the smallest grains seem to show a weak correlation, although two sites are an insignificant number and any causal link to the proposed impact event is unclear.

Table 4. Comparison of spherule abundances in the YDB layer reported by the three research groups at each of the three sites

Site	Firestone	Surovell	LeCompte
Blackwater Draw, NM	768	0	953
Topper, SC	87	0	260
Paw Paw Cove, MD	(not tested)	0	317

Note that the BWD value is an average for a 9.5-cm-thick interval of the YDB layer that includes both the D/C and D horizons.

Our comparative study has revealed a number of deficiencies in the protocol employed by Surovell et al. that are cumulative in their effect. The probability of successful spherule detection by that group was consequently reduced up to several orders of magnitude. In turn, this invalidates any conclusions by Surovell et al. about the three sites studied in this paper, and, most likely, the other four of their sites not addressed here. One exception may be their results from Agate Basin, WY where Surovell et al. reported significant coeval peaks in magnetic grains and spherules (<255/kg) in a layer they determined to be just above the YDB. For the Agate Basin site their protocol, although flawed, may still have been sensitive enough to detect larger spherules in high concentrations. Agate Basin has the largest spherule abundance reported by Surovell et al., which is located farther north than the other sites they studied. If accurate, their discovery of a spherule peak proximate to the YDB layer at the Agate Basin site may be an important contribution to YDB research, but more research is needed to confirm their results. We speculate that if one or more ET objects impacted near or on the Laurentide Ice Sheet as proposed, then spherule size and abundance should increase with proximity to the hypothesized impact site. This trend may be reflected in the results from Agate Basin. Alternately, it may simply be an enhancement due to local environmental processes.

Conclusions

Regarding the Surovell et al. study, our analyses indicate that YDB spherule abundances at three sites examined are consistent with those reported by Firestone et al. and inconsistent with those reported by Surovell et al. We conclude that any numerical differences between our results and those of Firestone et al. are within normal variation. The prescribed protocol produces reliably quantifiable results.

Our work indicates that Surovell et al., did not follow three of the most critical elements of the Firestone et al. protocol: (*i*) size-sorting of the magnetic fraction; (*ii*) the examination of sufficient amounts of magnetic material; and (*iii*) examination of candidate spherules by SEM and EDS. The result of these omissions was a methodology whose sensitivity was inadequate to detect significant numbers of spherules in any stratum, except perhaps those with abundant large spherules as may be the case in Agate Basin. We emphasize that future independent investigators testing for the presence or absence of YDB magnetic spherules include as standard procedure rigorous size-sorting as well as SEM/EDS analyses. At all three sites tested, grain size-sorting using a 53-μm screen greatly improved the ratio of spherules to distractor-grains, profoundly reducing the difficulties in searching, identifying, and accurately counting these small objects.

For magnetic grains, peaks in the total magnetic grain density at the three sites are not reliably correlated with the peaks in spherules or the onset of the Younger Dryas. This is consistent with the results reported by Surovell et al. However, a peak in the smallest (<53 μm) size portion of the magnetic grains does appear to have a weak correlation with YDB strata at TPR and BWD, perhaps indicative of some as-yet-unexplained depositional process operating at that time.

Microspherules at all three sites are morphologically and geochemically similar, averaging about 30 μm. Their chemical composition varies from aluminosilicate glass to magnetite to titanomagnetite. With the exception of one magnetic spherule

that is highly enriched in rare earth elements, the compositions of YDB spherules are similar to terrestrial metamorphic rocks and differ significantly from those formed by cosmic or authigenic processes. Volcanic and anthropogenic sources are considered unlikely.

Regarding a potential human population decline, our results from the TPR quarry site demonstrate that the spherule-enriched YDB layer approximately coincides with the start of multi-century hiatus in activity of this Clovis quarry. These results, combined with those from BWD and PPC, are consistent with a population decline that was coeval with the YDB event as previously proposed.

The scope of our study was limited to considering only the identification, occurrence, and nature of YDB magnetic spherules and the possible implications. Our results are consistent with, but do not prove, that a previously proposed cosmic impact occurred at 12.9 ka B.P. (the YDB impact hypothesis). The ultimate source of the magnetic microspherules in YDB sediment remains a mystery warranting further investigation.

Methods

The protocol we used here for extracting the magnetic fraction and the separation and identification of magnetic spherules was essentially the same as that used by Firestone et al. and improved by Israde-Alcantara et al. (4 and *SI Appendix* therein). Initial detection of candidate microspherules was made using an optical microscope to scan aliquots of approximately 10 mg scattered uniformly across a white microscope slide at a magnification of 130–150 power. There were some modifications as follows: (*i*) we used the strongest recommended NdFeB magnet (grade 52); (*ii*) we captured any grains small enough to be suspended on the surface of the liquid in which the magnetic fraction was dispensed by decanting the liquid through multiple 20-μm mesh filters and recovered the trapped residue in each; (*iii*) we found it useful to, and highly recommend, examining sectioned spherules to compare interior and exterior compositions; and (*iv*) we used a smaller-than-recommended screen mesh size (53-μm grid spacing) because it became evident that spherule detection and counting would be greatly facilitated by additional size-sorting (extra screens) to isolate smaller grain sizes. By using the smaller mesh size we were able to obtain spherule results that were consistent with those of Firestone et al. while using similar sized aliquots as Surovell et al.

All EDS data were collected by an Oxford Si(Li) X-ray detector with a 4Pi Universal Spectral Engine pulse processor. Since samples of this type that had been previously analyzed by other authors using more sensitive techniques (1, 5, 36, 38) and had been found to contain only metallic oxides, our analyses assume that all of the metallic elements are oxidized. The quantities of the various elements were determined by standardless EDS analysis and then converted to oxides by stoichiometry.

ACKNOWLEDGMENTS. Our thanks to Joanne Dickinson, who collected the BWD sediment, and Darrin Lowery, who facilitated collection of the Maryland sample. We are also grateful for the excellent work of our anonymous reviewers and for Ted Bunch and Allen West, who offered technical advice for this project.

1. Firestone RB, et al. (2007) Evidence for an extraterrestrial impact 12,900 years ago that contributed to the megafaunal extinctions and the Younger Dryas cooling. *Proc Natl Acad Sci USA* 106:16016–16021.
2. Kennett DJ, et al. (2009) Shock-synthesized hexagonal diamonds in Younger Dryas boundary sediments. *Proc Natl Acad Sci USA* 106:12623–12628.
3. Kennett DJ, et al. (2009) Nanodiamonds in the Younger Dryas boundary sediment layer. *Science* 323:94.
4. Israde-Alcántara I, et al. (2012) Evidence from Central Mexico supporting the Younger Dryas extraterrestrial impact hypothesis. *Proc Natl Acad Sci USA* 109:E738–E747.
5. Bunch TE, et al. (2012) Very high-temperature impact melt products as evidence for cosmic airbursts and impacts 12,900 years ago. *Proc Natl Acad Sci USA* 109: E1903–E1912.
6. Puffer JH, Russell EWB, Rampino MR (1980) Distribution and origin of magnetite spherules in air, waters, and sediments of the greater New York City area and the North Atlantic Ocean. *J Sediment Petrol* 50:247–256.
7. Brownlee DE (1981) *The Sea: Ideas and Observations on Progress in the Study of the Seas*, ed C Emiliani (Interscience, New York), pp 733–762.
8. Koeberl C (1990) The geochemistry of tektites: An overview. *Tectonophysics* 171:405–422.
9. Genge MJ (2008) Micrometeorites and their implications for meteors. *Earth Moon Planets* 102:525–535.
10. Simonson BM, Glass BP (2004) Spherule layers–records of ancient impacts. *Annu Rev Earth Planet Sci* 32:329–361.
11. Hodge PW, Wright FW (1964) Studies of particles for extraterrestrial origin 2. A comparison of microscopic spherules of meteoritic and volcanic origin. *J Geophys Res* 68:2449–2454.
12. Puffer JH (1974) Magnetite spherules in Miocene versus recent sands of New Jersey. *Meteoritics* 9:281–288.
13. Poppe T, Güttler C, Springborn T (2010) Thermal metamorphoses of cosmic dust aggregates: Experiments by furnace, electrical gas discharge, and radiative heating. *Earth, Planets Space* 62:53–56.
14. Haynes CV, Jr, Boerner J, Domanik D, Bellenger J, Goreva J (2010) The Murray Springs Clovis site, Pleistocene extinction, and the question of extraterrestrial impact. *Proc Natl Acad Sci USA* 107:4010–4015.
15. Mahaney WC, et al. (2010) Evidence from the northwestern Venezuelan Andes for extraterrestrial impact: The black mat enigma. *Geomorphology* 116:48–57.
16. Fayek M, Anovitz LM, Allard LF, Hull S, Haynes CV, Jr (2012) Framboidal iron oxide: Chondrite-like material from the black mat, Murray Springs, Arizona. *Earth Planet Sci Lett* 319–320:251–258.
17. Pigati JS, et al. (2012) Accumulation of "impact markers" in desert wetlands and implications for the Younger Dryas impact hypothesis. *Proc Natl Acad Sci USA* 109:7208–7212.
18. Surovell TA, et al. (2009) An independent evaluation of the Younger Dryas extraterrestrial impact hypothesis. *Proc Natl Acad Sci USA* 104:18155–18158.
19. Pinter N, et al. (2011) The Younger Dryas impact hypothesis: A requiem. *Earth-Sci Rev* 106:247–264.
20. Anderson DG, Goodyear AC, Kennett J, West A (2011) Multiple lines of evidence for possible human population decline/settlement reorganization during the early Younger Dryas. *Quat Int* 242:570–583.
21. Waters MR, Forman SL, Stafford TW, Jr, Foss J (2009) Geoarchaeological investigations at the Topper and Big Pine Tree sites, Allendale County, South Carolina. *J Archaeol Sci* 36:1300–1311.
22. Goodyear AC, Steffy K (2003) Evidence of a Clovis occupation at the Topper Site, 38AL23, Allendale County, South Carolina. *Curr Res Pleistocene* 20:23–25.
23. Lowery D (1989) The Paw Paw Cove Paleoindian site complex, Talbot County, Maryland. *Archaeology of Eastern North America* 17:143–163.
24. Lowery DL, O'Neal MA, Wah JS, Wagner DP, Stanford DJ (2010) Late Pleistocene upland stratigraphy of the western Delmarva Peninsula, USA. *Quat Sci Rev* 29:1472–1480.
25. Zagurski AM, Ivanov AV, Shoba SA (2009) Submicromorphology of soil magnetic fractions. *Eurasian Soil Sci* 42:1144–1052.
26. Brownlee DE, Bates B, Schramm L (1997) The elemental composition of stony cosmic spherules. *Meteorit Planet Sci* 32:157–175.
27. Orris GJ, Grauch RI (2002) *Rare Earth Element Mines, Deposits and Occurrences* USGS Open File Report 02-189.
28. Nakamura N, Masuda A (1973) Chondrites with peculiar rare-earth patterns. *Earth Planet Sci Lett* 19:429–437.
29. Boynton WV (1975) Fractionation in the solar nebula: Condensation of yttrium and the rare earth elements. *Geochim Cosmochim Acta* 39:569–584.
30. Evenson NM, Hamilton PJ, O'nions RK (1978) Rare-earth abundances in chondritic meteorites. *Geochim Cosmochim Acta* 42:1199–1212.
31. Mehta A, Barker GC, Luck JM (2008) Cooperativity in sandpiles: Statistics of bridge geometries. *Proc Natl Acad Sci USA* 105:8244–8249.
32. Duncan J, Humphreys GW (1989) Visual search and stimulus similarity. *Psychol Rev* 96:433–458.
33. Treisman A, Gelade G (1980) A feature integration theory of attention. *Cogn Psychol* 12:97–136.
34. Wolfe JM, van Wert MJ (2010) Varying target prevalence reveals two dissociable decision criteria in visual search. *Curr Biol* 20:121–124.
35. Treisman A, Gormican S (1988) Feature analysis in early vision: Evidence from search asymmetries. *Psychol Rev* 95:15–48.
36. Bi D (1993) Magnetic spherules from Pleistocene sediments in Alberta, Canada. *Meteoritics* 29:88–93.
37. Lougheed MS (1966) A classification of extraterrestrial spherules found in sedimentary rock and till. *Ohio J Sci* 66:274–283.
38. Zbik M (February 15, 1984) Morphology of the outermost shells of the Tunguska back magnetic spherules. *Proceedings of the Fourteenth Lunar and Planetary Science Conference, J Geophys Res*, 89 pp:B605–B611.
39. Marini F, Raukas A, Tiirmaa R (2004) Magnetic fines from the Kaali impact site (Holocene, Estonia). *Geochem J* 38:107–120.
40. Szöör G, et al. (2001) Magnetic spherules: Cosmic dust or markers of a meteoritic impact? *Nucl Instrum Methods Phys Res B* 181:557–562.
41. Taylor S, Lever JH, Harvey RP (2000) Numbers, types, and compositions of an unbiased collection of cosmic spherules. *Meteorit Planet Sci* 35:651–666.
42. USSG (2001) *Geochemistry of soils in the US from the PLUTO database*.
43. Haynes CV, Jr, et al. (1999) A Clovis well at the type site 11500 B.C.: The oldest prehistoric well in America. *Geoarchaeology* 14:455–470.
44. Befell J, Decker CL, Fiedel S, Shellenhamer J (2009) *Through the Great Valley and into the Mountains Beyond*, (National Park Service, National Capital Region, Washington, DC), Vol 1.
45. Buchanan B, Collard M, Edinborough K (2008) Paleoindian demography and the extraterrestrial impact hypothesis. *Proc Natl Acad Sci USA* 105:11651–11654.
46. Holliday VT, Meltzer DJ (2010) The 12.9-ka ET impact hypothesis and North American Paleoindians. *Curr Anthrop* 51:575–607.

Supporting Information Corrected October 24, 2012

Independent Evaluation of Conflicting Microspherule Results from Different Investigations of the Younger Dryas Impact Hypothesis

SUPPORTING INFORMATION.

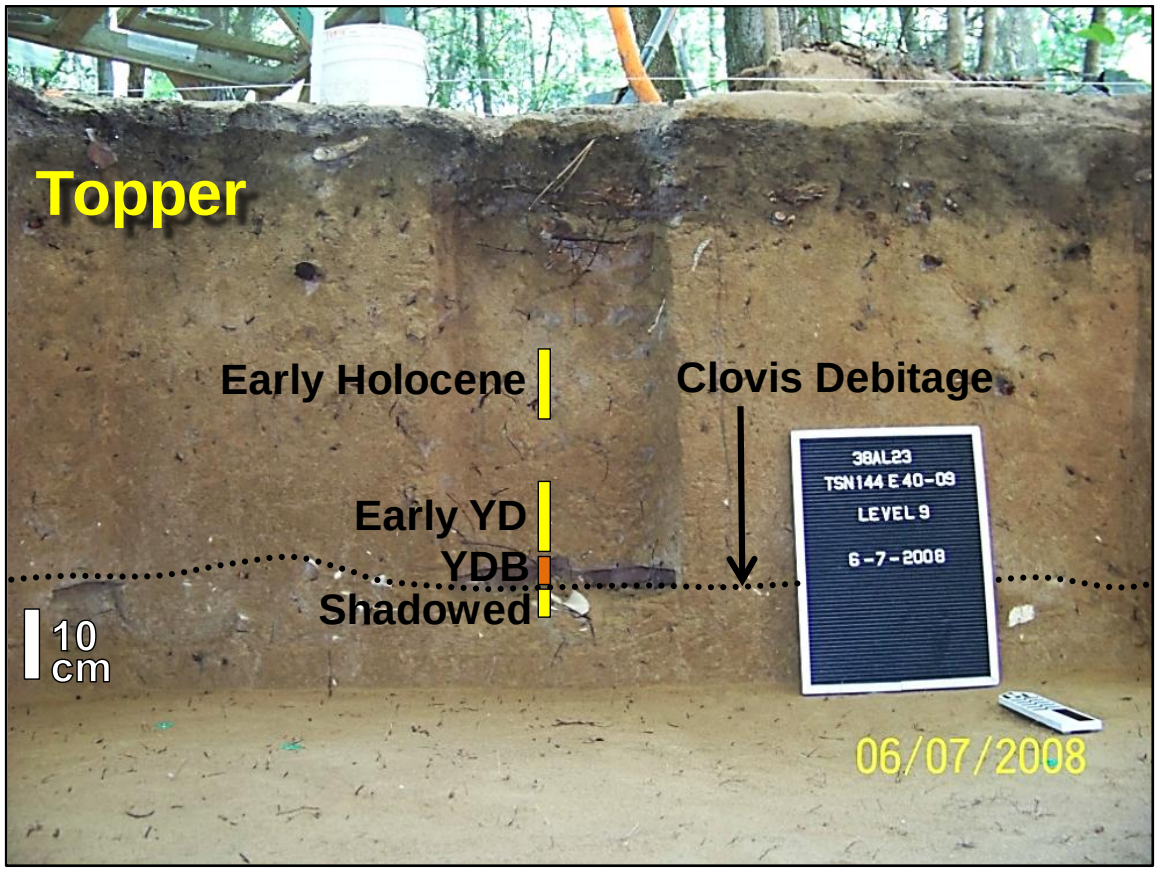

SI Fig. 1. Topper sampling site showing YDB layer as dotted black line, atop Clovis debitage. YDB sample location at orange bar; other samples at yellow bars.

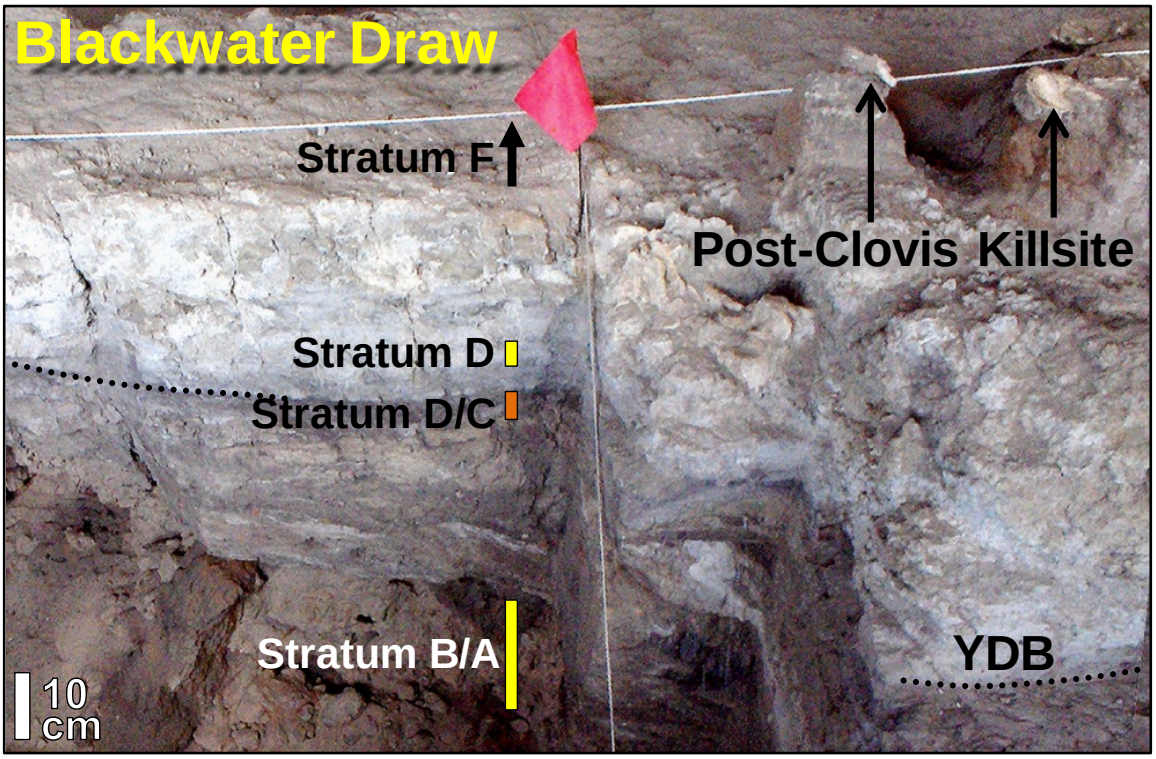

SI Fig. 2. BWD sampling site showing YDB layer as dotted line. YDB sample location at orange bar; other samples at yellow bars. Stratum F has been excavated and is not visible in this photo. Black arrows point to bones from a post-Clovis bison kill dating to many hundreds of years after 12,900 years ago. There are no artifacts known in the intervening strata.

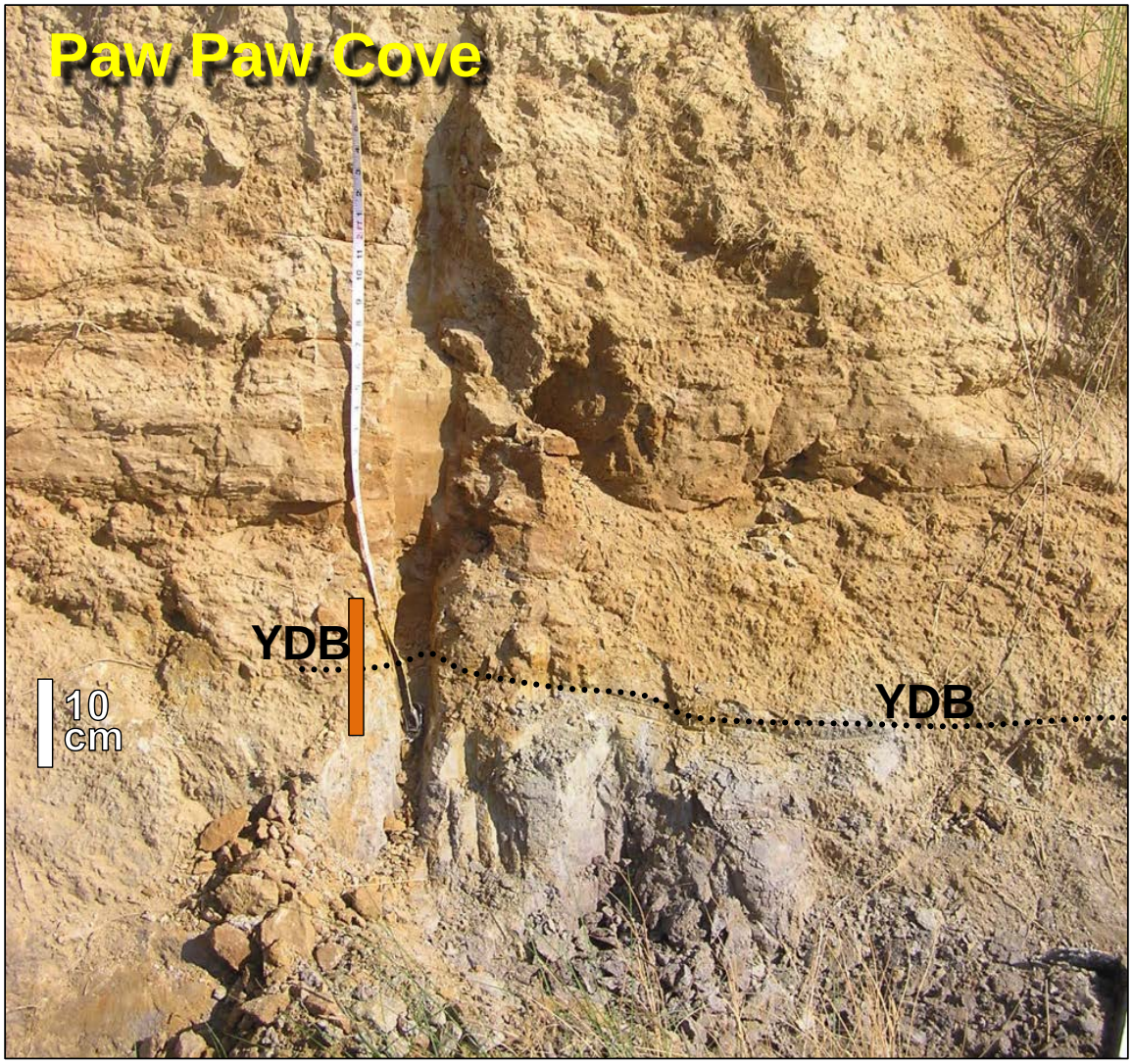

SI Fig. 3. PPC sampling site showing YDB layer as dotted line. YDB sample location at orange bar.

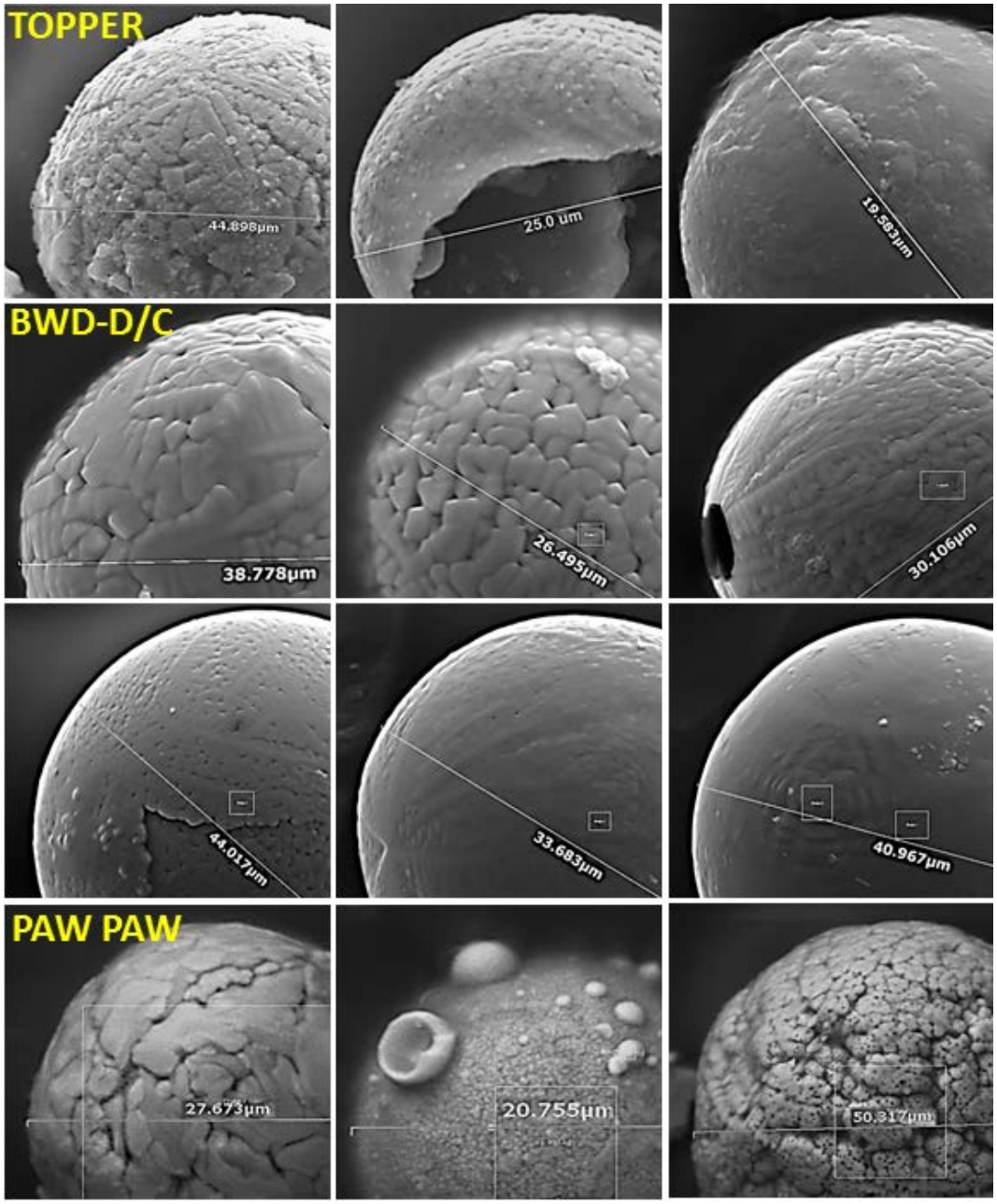

SI Fig. 4. YDB spherules displaying some of the wide range of surface microstructures indicative of melting and rapid quenching. Top three are from above the debitage layer at Topper. Middle six are from Blackwater Draw (BWD) in the D/C layer. Bottom three are from Paw Paw Cove (PPC).

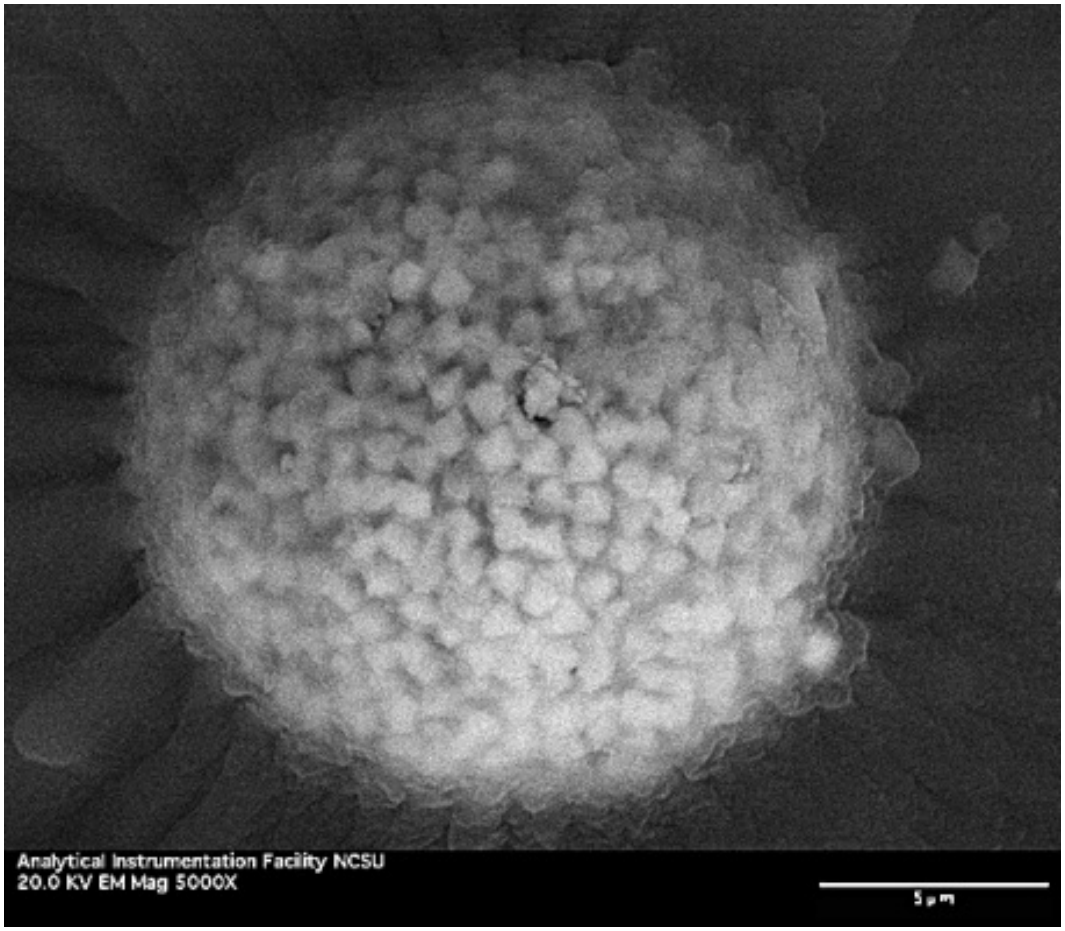

SI Fig. 5. SEM Micrograph showing a Topper 17-µm-diameter framboidal spherule. At these three sites, framboids are morphologically different but chemically indistinguishable from the apparently melted microspherules described in the foregoing. On the other hand, Israde et al. (2012) reported that sulfur-rich framboids from Lake Cuitzeo, Mexico are chemically different from the ones we observed.

SI Table 1. Oxide percentages of microspherules analyzed from Topper, SC.

	Layer and spherule #	Microns	FeO	Al_2O_3	MgO	CaO	SiO_2	K_2O	Na_2O	TiO_2	P_2O_5	MnO	Cr_2O_3	NiO	SO_3
1	TU2-YDB-Sph-1-110505	33	8.66	24.64	0.02	0.45	63.78	1.64	0.01	0.74	0.00	0.01	0.00	0.03	0.01
2	TU2-YDB-Sph-2-110505-28mic	28	66.53	14.87	0.07	0.53	11.58	1.74	0.41	0.64	3.06	0.22	0.00	0.00	0.35
3	TU2-YDB-Sph-3-100514	17	88.64	6.15	0.00	0.63	4.58	0.00	0.00	0.00	0.00	0.00	0.00	0.00	0.00
4	TU2-YDB-Sph-4-110505	26	96.31	1.86	0.00	0.38	0.45	0.00	0.00	0.68	0.00	0.00	0.18	0.00	0.14
5	TU2-YDB-Sph-5-110505	45	75.34	12.39	0.81	0.15	9.99	0.01	0.33	0.92	0.00	0.02	0.01	0.03	0.00
6	TU2-YDB-Sph-6-110505	25	91.78	3.60	0.47	0.25	2.96	0.20	0.65	0.01	0.00	0.00	0.01	0.00	0.07
7	TU2-YDB-Sph-8-110506	20	96.86	1.51	0.00	0.39	0.47	0.00	0.00	0.22	0.02	0.00	0.42	0.00	0.11
8	TU2-YDB-Sph-9-110506	30	54.25	16.60	0.22	0.58	27.29	0.50	0.31	0.23	0.00	0.00	0.02	0.00	0.00
9	TU2-YDB-Sph-17-110314	23	49.00	4.53	4.98	0.07	3.48	0.13	1.52	34.98	0.98	0.33	0.01	0.00	0.00
10	TU2-YD-Sph-1-110314	26	37.38	6.63	1.55	0.07	3.30	0.00	0.86	47.02	0.62	2.55	0.01	0.00	0.00
11	TU2-YD-Sph-2-110314	48	4.70	39.09	0.57	0.08	54.56	0.25	0.44	0.01	0.28	0.00	0.01	0.01	0.00
	AVERAGES (25):	**29**	**60.86**	**11.99**	**0.79**	**0.33**	**16.59**	**0.41**	**0.41**	**7.77**	**0.45**	**0.28**	**0.06**	**0.01**	**0.06**

SI Table 2. Oxide percentages of microspherules analyzed from Blackwater Draw, NM.

	Layer and spherule #	Mic.	FeO	Al_2O_3	MgO	CaO	SiO_2	K_2O	Na_2O	TiO_2	P_2O_5	MnO	Cr_2O_3	NiO	SO_3
1	BWD-DC-Sph-1-100514-33mic	33	57.63	1.46	0.18	1.90	6.32	1.81	8.92	0.95	0.11	4.17	2.10	2.32	12.13
2	BWD-DC-Sph-1-100621-29mic	29	94.08	2.00	0.63	0.20	1.72	0.00	0.86	0.08	0.27	0.15	0.00	0.01	0.00
3	BWD-DC-Sph-2-100621-33mic	33	93.74	2.18	0.88	0.21	1.77	0.01	0.93	0.05	0.00	0.00	0.02	0.00	0.21
4	BWD-DC-Sph-3-100621-34mic	34	93.15	2.83	0.96	0.07	1.56	0.10	1.22	0.00	0.00	0.11	0.00	0.00	0.00
5	BWD-DC-Sph-4-100621-37mic	37	87.74	2.69	1.22	0.13	4.52	0.00	1.03	0.02	0.10	2.10	0.15	0.04	0.26
6	BWD-DC-Sph-1-110314-36mic	36	65.35	2.54	2.13	2.32	25.67	0.05	1.09	0.07	0.17	0.00	0.00	0.00	0.60
7	BWD-DC-Sph-2-110314-30mic	30	97.15	1.07	0.00	0.25	1.00	0.00	0.00	0.01	0.34	0.18	0.00	0.00	0.00
8	BWD-DC-Sph-3-110314-44mic	44	91.71	1.39	1.02	0.27	2.81	0.02	0.56	0.00	0.41	1.78	0.02	0.01	0.00
9	BWD-DC-Sph-4-110314-27mic	27	94.42	1.62	0.99	0.28	1.51	0.10	0.65	0.00	0.21	0.21	0.00	0.01	0.00
10	BWD-DC-Sph-5-110314-34mic	34	95.39	2.16	0.50	0.21	0.84	0.00	0.32	0.01	0.17	0.38	0.00	0.02	0.00
11	BWD-DC-Sph-6-110314-26mic	26	95.48	1.05	0.45	0.37	1.18	0.00	0.47	0.22	0.31	0.44	0.02	0.01	0.00
12	BWD-DC-Sph-7-110314-31mic	31	95.72	0.95	0.87	0.24	1.17	0.02	0.54	0.11	0.36	0.00	0.00	0.02	0.00
13	BWD-DC-Sph-8-110314-39mic	39	94.91	1.25	0.90	0.19	1.54	0.00	0.52	0.00	0.26	0.43	0.00	0.00	0.00
14	BWD-DC-Sph-8-110314-39mic	39	94.07	1.39	1.04	0.20	1.98	0.00	0.77	0.00	0.21	0.34	0.00	0.00	0.00
15	BWD-DC-Sph-9-110314-41mic	41	95.70	1.35	0.81	0.28	1.03	0.01	0.51	0.02	0.25	0.03	0.00	0.01	0.00
16	BWD-DC-Sph-9-110314-41mic spot	41	93.46	1.86	1.20	0.17	1.82	0.05	1.00	0.02	0.34	0.00	0.00	0.08	0.00
17	BWD-DC-Sph-10-110314-30mic	30	96.59	0.85	0.44	0.27	1.22	0.06	0.27	0.01	0.08	0.21	0.00	0.00	0.00
18	BWD-D-Sph-1-110314-32mic spot 1	32	94.85	1.93	0.68	0.25	1.46	0.00	0.43	0.08	0.25	0.06	0.01	0.00	0.00
19	BWD-D-Sph-1-110314-32mic-spot 2	32	89.79	2.83	1.59	0.27	2.95	0.13	1.43	0.55	0.29	0.07	0.00	0.10	0.00
20	BWD-D-Sph-2-110314-30mic spot 1	30	96.72	1.22	0.03	0.29	1.09	0.06	0.00	0.09	0.00	0.31	0.00	0.00	0.19
21	BWD-D-Sph-2-110314-30mic spot 2	30	96.37	1.17	0.09	0.27	1.56	0.02	0.00	0.09	0.00	0.28	0.00	0.00	0.15
22	BWD-D-Sph-3-110314-35mic spot 1	35	92.56	2.30	1.00	0.33	1.61	0.10	0.68	0.01	0.43	0.96	0.00	0.02	0.00
23	BWD-D-Sph-3-110314-35mic spot 2	35	93.29	2.00	0.61	0.37	1.89	0.00	0.51	0.00	0.32	0.99	0.00	0.02	0.00
24	BWD-D-Sph-4-110314-34mic	34	94.99	1.51	0.87	0.28	1.24	0.13	0.64	0.01	0.07	0.25	0.00	0.01	0.00
25	BWD-D-Sph-5-110314-39mic	39	93.17	2.01	1.21	0.12	2.14	0.06	0.69	0.02	0.33	0.25	0.00	0.00	0.00
26	BWD-D-Sph-6-110314-23mic	23	94.21	1.72	0.94	0.23	1.58	0.00	0.87	0.00	0.31	0.14	0.00	0.00	0.00
27	BWD-D-Sph-7-110314-29mic	29	95.12	1.63	0.83	0.12	1.25	0.04	0.60	0.01	0.24	0.16	0.00	0.00	0.00
28	BWD-D-Sph-8-110314-33mic spot 1	33	93.55	2.03	1.22	0.31	1.48	0.00	0.98	0.00	0.20	0.19	0.00	0.04	0.00
29	BWD-D-Sph-8-110314-33mic spot 2	33	93.51	1.81	1.42	0.33	1.24	0.09	0.79	0.00	0.31	0.50	0.00	0.00	0.00
30	BWD-D-Sph-9-110314-49mic spot 1	49	96.12	1.12	0.47	0.14	1.29	0.08	0.28	0.03	0.24	0.23	0.00	0.00	0.00
31	BWD-D-Sph-9-110314-49mic spot 2	49	96.83	0.75	0.45	0.15	0.90	0.00	0.42	0.04	0.26	0.20	0.00	0.00	0.00
32	BWD-D-Sph-10-110314-20mic	20	91.79	1.88	1.10	0.55	3.08	0.00	0.91	0.00	0.62	0.04	0.00	0.03	0.00
33	BWD-D-Sph-11-110314-35mic	35	96.63	1.18	0.45	0.31	0.76	0.00	0.45	0.06	0.15	0.01	0.00	0.00	0.00
34	BWD-D-Sph-12-110314-27mic	27	93.68	1.68	0.90	0.27	1.01	0.07	0.77	0.00	0.36	1.23	0.01	0.02	0.00
35	BWD-D-Sph-13-110314-28mic	28	96.76	1.51	0.17	0.09	0.68	0.00	0.28	0.01	0.18	0.27	0.02	0.00	0.03
36	BWD-D-Sph-14-110314-29mic	29	93.54	1.85	1.08	0.33	1.77	0.09	0.82	0.01	0.24	0.27	0.00	0.00	0.00
37	BWD-D-Sph-15-110314-34mic spot 1	34	37.12	2.42	1.59	0.13	3.33	0.03	1.02	53.89	0.20	0.26	0.01	0.00	0.00
38	BWD-D-Sph-15-110314-34mic spot 2	34	36.49	1.10	0.27	0.25	2.29	0.03	0.43	57.70	0.26	0.58	0.00	0.00	0.60
39	BWD-D-Sph-15-110314-34mic spot 3	34	25.47	5.16	2.58	0.53	14.06	0.37	0.82	50.79	0.00	0.05	0.01	0.00	0.16
40	BWD-D-Sph-16-110314-31mic	31	96.60	0.79	0.21	0.16	1.12	0.00	0.30	0.01	0.47	0.23	0.01	0.00	0.10
41	BWD-D-Sph-17-110314-23mic	23	91.71	1.39	1.02	0.27	2.81	0.02	0.56	0.00	0.41	1.78	0.02	0.01	0.00
42	BWD-D-Sph-18-110314-41mic spot 1	41	59.86	2.19	2.69	0.14	1.68	0.03	0.02	32.65	0.33	0.12	0.00	0.00	0.29
43	BWD-D-Sph-18-110314-41mic spot 2	41	55.29	3.41	4.68	0.38	2.99	0.00	0.78	31.95	0.37	0.07	0.03	0.02	0.03
44	BWD-D-Sph-18-110314-41mic spot 3	41	48.19	4.41	6.77	0.17	4.35	0.00	1.17	34.52	0.34	0.02	0.01	0.05	0.00
45	BWD-D-Sph-19-110314-25mic	25	96.51	0.90	0.12	0.12	1.43	0.01	0.34	0.44	0.13	0.00	0.00	0.00	0.00
46	BWD-D-Sph-20-110314-48mic	48	96.29	0.83	0.91	0.09	0.90	0.03	0.51	0.04	0.27	0.13	0.00	0.00	0.00
47	BWD-D-Sph-21-110314-34mic spot 1	34	94.10	1.57	0.44	0.27	1.79	0.11	0.68	0.01	0.41	0.49	0.00	0.00	0.13
48	BWD-D-Sph-22-110314-37mic spot 1	37	98.63	0.22	0.00	0.17	0.84	0.01	0.00	0.08	0.00	0.05	0.00	0.00	0.00
49	BWD-D-Sph-22-110314-37mic spot 2	37	45.22	2.37	6.30	0.01	4.27	0.02	1.33	39.41	0.00	1.01	0.05	0.01	0.00
50	BWD-D-Sph-22-110314-37mic spot 3	37	41.88	6.80	4.96	0.58	15.48	0.22	0.85	27.00	0.04	1.95	0.03	0.00	0.21
51	BWD-D-Sph-22-110314-37mic spot 4	37	73.37	3.09	3.43	0.04	5.28	0.01	1.42	12.26	0.37	0.59	0.00	0.00	0.14
52	BWD-D-Sph-23-110314-25mic	25	95.95	0.69	0.53	0.20	1.73	0.06	0.33	0.03	0.10	0.31	0.00	0.03	0.04
	AVERAGES (52):	**34**	**85.05**	**1.89**	**1.27**	**0.31**	**2.90**	**0.08**	**0.80**	**6.60**	**0.23**	**0.47**	**0.05**	**0.06**	**0.29**

SI Table 3. Oxide percentages of microspherules analyzed from Paw Paw Cove, MD. Note REEs for one spherule.

	Layer and spherule #	Mic.	FeO	Al_2O_3	MgO	CaO	SiO_2	K_2O	Na_2O	TiO_2	P_2O_5	MnO	Cr_2O_3	NiO	SO_3	La_2O_3	CeO_2	Pr_6O_{11}	Nd_2O_3
1	PPC-YDB-Sph-1-100707-17mic	17	42.4	2.89	1.25	0.43	1.87	0.2	2.67	45.9	0.97	0.96	0.00	0	0.5	0.00	0.00	0.00	0.00
2	PPC-YDB-Sph-2-100707-21mic	21	48.24	4.79	6.11	0.12	2.66	0.03	4.90	0.03	0.00	0.84	0.12	0.01	0.21	10.10	21.83	0.00	0.00
3	PPC-YDB-Sph-2-100707-21mic Rim	21	24.00	7.37	2.40	0.72	4.85	0.13	1.18	1.07	0.06	0.38	0.00	0.00	2.17	22.17	27.56	3.72	2.21
4	PPC-YDB-Sph-2-100707 21mic Bulge	21	47.23	5.07	5.05	0.26	3.68	0.04	5.94	0.39	0.04	0.00	0.00	0.03	0.86	9.59	21.81	0.00	0.00
5	PPC-YDB-Sph-3-100707 36mic	36	22.89	6.82	0.73	0.25	2.55	0.05	0.64	52.23	0.28	13.20	0.01	0.00	0.35	0.00	0.00	0.00	0.00
6	PPC-YDB-Sph-4-100707 50mic	50	41.00	6.83	0.67	0.12	2.59	0.05	0.61	47.5	0.12	0.01	0.01	0.00	0.45	0.00	0.00	0.00	0.00
7	PPC-YDB-Sph-5-100707 28mic	28	39.22	3.64	0.00	0.35	2.14	0.22	0.00	50.85	0.67	2.91	0.00	0.00	0.00	0.00	0.00	0.00	0.00
8	PPC-YDB-Subround-100707-27mic	27	51.10	3.42	1.80	0.27	2.77	0.08	0.29	39.71	0.02	0.29	0.05	0.05	0.15	0.00	0.00	0.00	0.00
	AVERAGES (8):	**27**	**39.51**	**5.10**	**2.25**	**0.32**	**2.89**	**0.10**	**2.03**	**29.72**	**0.27**	**2.32**	**0.02**	**0.01**	**0.58**	**5.23**	**8.90**	**0.47**	**0.28**

SI Table 4. Table below provides a summary comparison of each group's application of the Firestone et al. protocol.

Protocol Measure	Firestone et al. (2007) + 08/07/2007 Protocol	Surovell et al. (2009)	LeCompte et al. (2010)
NdFeB Magnet Strength	N-42	N-42	N-52*
Sediment Sample Amount	0.5 - 1.0 kg	0.2 to 0.5 kg	0.2 - 0.3 kg
Magnet's Plastic bag thickness	4 mil	4 mil	2-3 mil
Magnetic Grain Extraction Cycles	5 - 10 immersions	Up to 30 @ 1-minute immersions	20 @ 45-second immersions
Magnetic Grain Rinse Cycles **	As needed	Series of baths as needed	10 @ 45-second immersions with 20-µm paper filtration
Microscope Magnification (power x)	100-150x/150x	100x/100x***	130x/180x****
Sieve for Size-Sorting	Recommended <150 µm	1 mm	250 & 53 µm
Magnetic Grain -- total aliquot size	100 - 200 mg, up to total magnetic fraction	10-40 mg	20-40 mg of the <53-µm magnetic fraction
Spherule Visual Characteristics	Unfaceted; usually spherical; usually reflective surface	Unfaceted; perfectly spherical; only highly reflective surface	Unfaceted; nearly all spherical; mostly highly reflective surface

*N-42 exerts about 75% the magnetic force of N-52

** Protocol did not provide explicit instructions regarding a rinse cycle

***300x using electronic pixel zoom (pixel density increase)

**** Scanning at >130x was necessary to detect spherules <15-20 µm diameter

SI Table 5. Topper quarry. Shows number and type of artifacts found during and after Clovis times (data from Anderson et al., 2011).

	Site#	St.	Clovis	Post Clovis	Type of Site
Topper Clovis Quarry	38AI23	SC	4 Clovis points	1 Instrument-assist. pt.	Quarry, Workshop, Habitation
			170 Preforms		
			257 Blades		
			22 Blade Cores		